JMJD-1.2/PHF8 controls axon guidance by regulating Hedgehog-like signaling

Alba Redo Riveiro[1,2,5¶], Luca Mariani[1,2,5¶], Emily Malmberg[1,2], Pier Giorgio Amendola[1,2], Juhani Peltonen[3], Garry Wong[4] and Anna Elisabetta Salcini[1,2,*]

[1] Biotech Research & Innovation Centre (BRIC), University of Copenhagen, Copenhagen, Denmark

[2] Centre for Epigenetics, University of Copenhagen, Copenhagen, Denmark

[3] A. I. Virtanen Institute for Molecular Sciences, Department of Neurobiology, University of Eastern Finland, Kuopio, Finland

[4] Faculty of Health Sciences, University of Macau, Macau, China

[5] Current Address: The Danish Stem Cell Center (DanStem), University of Copenhagen, Copenhagen, Denmark

[*] Author for correspondence: E-mail: lisa.salcini@bric.ku.dk

[¶]These authors contributed equally to this work.

Key words: Epigenetics, histone demethylase, neuronal development, axon guidance, Hedgehog signaling, *C. elegans*

Summary statement

The authors propose a novel function of JMJD-1.2/PHF8 in axon guidance and provide the first evidence that Hedgehog–like signaling acts in *Caenorhabditis elegans* as a neurodevelopmental cue.

Abstract

Components of the KDM7 family of histone demethylases are implicated in neuronal development and one member, PHF8, is also found mutated in cases of X-linked mental retardation. However, how PHF8 regulates neurodevelopmental processes and contributes to the disease is still largely missing. Here we show that the catalytic activity of a PHF8 homolog in *Caenorhabditis elegans*, JMJD-1.2, is required non-cell autonomously for proper axon guidance. Loss of JMJD-1.2 deregulates the transcription of the Hedgehog-related genes *wrt-8* and *grl-16* whose overexpression is sufficient to induce the axonal defects. Deficiency of either *wrt-8* or *grl-16*, or reduced expression of homologs of genes promoting Hedgehog signaling restore correct axon guidance in *jmjd-1.2* mutant. Genetic and overexpression data indicate that Hedgehog-related genes act on axon guidance through actin remodelers. Thus, our study highlights a novel function of *jmjd-1.2* in axon guidance that may be relevant for the onset of X-linked mental retardation and provides compelling evidences of a conserved function of the Hedgehog pathway in *C. elegans* axon migration.

INTRODUCTION

The KDM7 family of histone demethylases, consisting of three members, KDM7A (KIAA1718), KDM7B (PHF8) and KDM7C (PHF2), is characterized by the presence of a C-terminal JmjC domain and a PHD finger domain at the N-terminal portion. The members of this family have been associated with neurodevelopmental processes (Kleine-Kohlbrecher et al., 2010; Qiu et al., 2010; Qi et al., 2010; Tsukada et al., 2010; Huang et al., 2010) and deletions or mutations of PHF8 are often identified in cases of X-linked mental retardation (XLMR) (Siderius et al., 1999; Laumonnier et al., 2005; Koivisto et al., 2007; Abidi et al., 2007; Loenarz et al., 2010; Redin et al., 2014), a highly heterogeneous group of inherited disorders characterized by impaired intellectual functions and cognitive abilities (Chiurazzi et al., 2004; Ropers and Hamel, 2005). While the JmjC domain of PHF8 catalyzes the removal of H3K9me2/me1 and H4K20me1, its PHD finger binds H3K4me3 and contributes to the demethylase activity of the protein at appropriate target sites (Feng et al., 2010, Kleine-Kohlbrecher et al., 2010; Liu et al., 2010). Several studies have shown that PHF8 is required to control the expression of neuronal genes (Kleine-Kohlbrecher et al., 2010; Qiu et al., 2010; Fortschegger et al., 2010; Fortschegger and Shiekhattar, 2011), however, how PHF8 controls specific aspects of neuronal development and functions that may be relevant for the onset of the cognitive disorders, remains poorly comprehended.

In mammals, the understanding of how specific factors orchestrate neurodevelopmental processes is challenged by the complexity of the nervous system, which consists of heterogeneous cellular populations comprised of billions of neurons. The nematode *Caenorhabditis elegans* instead is an excellent model to investigate these processes on a simpler and more tractable scale: its nervous system consists of 302 cells, whose morphology, function and connectivity have been extensively characterized (Sulston, 1983; White et al., 1986). Many chromatin regulators are conserved in *C. elegans* and important information regarding the role of these proteins in neuronal development has been recently achieved using this model system (Weinberg et al., 2013; Zheng et al., 2013; Mariani et al., 2016). PHF8 shares high homology with the *C. elegans* JMJD-1.2 protein, which retains both the JmjC and the PHD finger domains. However, the catalytic activity of JMJD-1.2 appears partially different compared to the mammalian counterpart, as several studies have shown its ability to demethylate not only H3K9me2, but also H3K27me2 and H3K23me2, both *in vitro* and *in vivo* (Kleine-Kohlbrecher et al., 2010; Lin et al., 2010; Vandamme et al., 2015). In agreement with

the role of PHF8 in neuronal processes, JMJD-1.2 is required for normal locomotion in *C. elegans*, highlighting the importance of this protein in the establishment of neuronal functionalities (Kleine-Kohlbrecher et al., 2010).

During the development of the nervous system, a multitude of attractive and repulsive cues orchestrate the migration of neuronal cells and the direction of their processes (Ayala et al., 2007; Robichaux and Cowan, 2014). In addition to well-characterized ligands (like netrins, slits, ephrins and semaphorins), a component of the Hedgehog family of morphogens, sonic Hedgehog (SHH), has been shown to regulate neural cell migration and axon guidance in vertebrates (Jarov et al., 2003; Bourikas et al., 2005; Sanchez-Camacho and Bovolenta, 2008; Hammond et al., 2009; Yam and Charron, 2013). Following synthesis and intracellular processing, Hedgehog ligands (Hh) are secreted by the combined action of receptors (i.e. Dispatched/DISP), diffuse in the extracellular matrix through the interaction with lipoproteins and proteoglycans (i.e. LRP2 and Glypican-6) and target cells expressing Patched receptors (PTCH1/PTCH2). The binding of Hh to Patched activates the signaling pathway in receiving cells by releasing Smoothened (SMO) inhibition and triggering a signal transduction cascade through the regulation of Fused (FU) and suppressor of Fused (SUFU). Ultimately, this leads to the activation of the transcription factors Gli, which control the expression of Hh target genes (Guerrero and Kornberg, 2014). Hh can also activate an alternative pathway (Jenkins, 2009), Gli- and, in some cases, SMO-independent, that leads to transcriptional-independent responses. Interestingly, this non-canonical Hh pathway regulates neural cell migration and axon guidance by modulating actin cytoskeleton reorganization (Bijlsma et al., 2007; Yam et al., 2009; Sasaki et al., 2010).

In the nematode, clear homologs of key components of the Hedgehog pathway, including Hh, SMO, FU and SUFU have not been identified. Instead, the *C. elegans* genome encodes an abundance of what are collectively known as Hedgehog-related proteins (i.e. WRT, GRL, GRD, QUA, HOG) based on their partial homology to domains found in the Hedgehog proteins (Bürglin and Kuwabara, 2006; Kolotuev et al., 2009). Other molecules of this signaling pathway appear conserved in *C. elegans*, and homologs of factors required for Hedgehog secretion (CHE-14, PTD-2/Dispatched), trafficking (GPN-1/Glypican-6, RIB-1/EXT1, RIB-2/EXTL3, LRP-1/LRP2, PHG-1/Gas1), Hedgehog receptors (PTC-1, PTC-3/Patched) and transcription factors responsible for mediating Hedgehog transcriptional activities (TRA-1/Gli1/3) are identified. Ablation of some components of the Hh pathway results in defects in molting and body morphology (Zugasti et al., 2005; Hao et al., 2006a), suggesting that, despite a considerable divergence, some Hedgehog functions are maintained in *C. elegans*.

Here, we show that the catalytic activity of JMJD-1.2 is required in the developing nervous system and hypodermis of *C. elegans* embryos to ensure correct axon guidance of specific neurons. Genome-wide analyses, in combination with genetic and overexpression studies, indicate that the defective axon guidance observed in *jmjd-1.2* mutants stems from the deregulated transcription of a set of genes, including two Hedgehog-related molecules. Genetic analyses indicate that the axon guidance defects identified in *jmjd-1.2* mutant animals or caused by ectopic expression of Hedgehog-related genes depend on actin remodelers, suggesting that the Hedgehog-like pathway controls axon guidance by regulating actin dynamics.

RESULTS

jmjd-1.2 mutant animals display neuronal defects

To gain insights into the role of JMJD-1.2 in the nervous system, we analyzed different axon guidance and neuronal cell migration events in the *jmjd-1.2* mutant allele *tm3713*, which carries an in-frame deletion that removes the region encoding the PHD finger domain (Kleine-Kohlbrecher et al., 2010; Lin et al., 2010). Although transcribed (Kleine-Kohlbrecher et al., 2010), the deleted locus results in loss of the JMJD-1.2 protein, as we and others could not detect JMJD-1.2 neither by western blot nor by immunofluorescence, suggesting that *tm3713* is probably a null mutant (Fig. 1A, B and Lin et al., 2010). Using a specific antibody, JMJD-1.2 appears expressed in many, if not all, nuclei (Fig. 1B and Fig. S1A), confirming the expression pattern identified analyzing the expression of a GFP-tagged JMJD-1.2 construct (Kleine-Kohlbrecher et al., 2010). By the use of transgenic animals carrying fluorescent markers for specific neurons, we found that loss of JMJD-1.2 led to the aberrant migration of axons projected by specific pairs of neurons, namely PVQs and HSNs. In wild-type animals, PVQ cellular bodies are located in the lumbar ganglia and their projections run along two distinct bundles of the ventral nerve cord. In *jmjd-1.2(tm3713)* mutant animals, PVQ neurons are born and positioned correctly, but their axons fail to maintain the correct trajectory and aberrantly cross over the ventral midline in 22% of the population (Fig. 1C, D). A similar phenotype was identified in a null mutant generated by CRISPR (clustered regularly interspaced short palindromic repeats) system (Fig. S1B). Axonal defects were also observed in the HSN neurons (Table 1 and Fig. S1C, D). Occasionally, the HSN cellular bodies, normally located in the vulva region, were undermigrated, suggesting an additional role for *jmjd-1.2* in neuronal cell body positioning. Moreover, in *jmjd-1.2(tm3713)* mutants, the expression of the

evIs82b transgene, specifically expressed in DA/DB motoneurons, was often reduced in the body and projection of DB5 (Table 1 and Fig. S1E, F). Transgenic animals carrying constructs expressed in other neurons, however, showed normal patterning of axon migration (Table 1), suggesting that loss of *jmjd-1.2* does not affect the whole architecture of the nervous system.

jmjd-1.2 acts during embryogenesis in nervous system and hypodermis to ensure correct axon guidance

To study the functional role of JMJD-1.2 in axon guidance, we focused on the analysis of the PVQs, well-studied interneurons that fully develop during embryogenesis. To test whether the PVQ axonal defects observed in *jmjd-1.2* mutants occur in embryogenesis or during larval development, we analyzed the PVQ neurons of freshly hatched L1 mutant larvae. As shown in Fig. 2A, the penetrance of the phenotype at this stage was comparable to that of L4 animals, suggesting that the described defects arise during embryonic development and are not related to defective maintenance of the axon pathfinding (Aurelio et al., 2002; Pocock et al., 2008; Bénard et al., 2012).

Transgenic expression of a translational fusion between the *jmjd-1.2* genetic locus and GFP could rescue the PVQ defects observed in *tm3713*, confirming that the axon guidance phenotype is due to loss of JMJD-1.2 (Fig. 2B and Table S1). Previous studies have shown that *jmjd-1.2* is expressed at all developmental stages and in multiple tissues, including neurons, muscles, intestine and hypodermis (Kleine-Kohlbrecher et al., 2010), a spatial-temporal expression confirmed by immunostaining with a specific antibody (Fig. 1B). To uncover the focus-of-action of *jmjd-1.2* in the context of PVQ axon guidance, we re-expressed GFP-tagged JMJD-1.2 in *tm3713* background using a panel of tissue-specific promoters (Fig. 2C and S2, Table S1). We drove *jmjd-1.2* expression under the control of either *rab-3* (nervous system) or *dpy-7* (hypodermis) promoters and found significant rescue of PVQ defects in each case, although the rescuing effect was slightly enhanced by re-expressing JMJD-1.2 in both tissues simultaneously (Fig. 2C). In contrast, we could not rescue the phenotype by expressing *jmjd-1.2* under the *myo-3* (body wall muscle) promoter, showing that the presence of JMJD-1.2 in muscle cells is not required for axon guidance (Fig. 2C). In agreement with the requirement of JMJD-1.2 in multiple tissues, driving its expression in the PVQ or in the pioneer PVP neurons is not sufficient to restore the normal guidance of the PVQs, suggesting that JMJD-1.2 does not work cell-autonomously nor in PVPs (Fig. S3). All together, these data strongly suggest that JMJD-1.2 controls the guidance of the PVQs acting from both nervous system and hypodermis.

The JmjC and the PHD finger domains of JMJD-1.2 are essential for correct axon guidance

JMJD-1.2 is structured around two evolutionarily conserved domains: the JmjC domain and the H3K4me3-binding PHD finger (Kleine-Kohlbrecher et al., 2010; Lin et al., 2010). The JmjC domain of JMJD-1.2 has been shown to demethylate H3K9me2, H3K27me2 and H3K23me2 both *in vitro* and *in vivo* and, accordingly, increased signal of these post-translational modifications is found in the *tm3713* mutant strain (Kleine-Kohlbrecher et al., 2010; Lin et al., 2010; Vandamme et al., 2015). To test the relevance of JMJD-1.2 enzymatic activity in axon guidance, we mutagenized the JmjC domain (Fig. 3A) by substituting two conserved amino acids required for the catalytic activity (Klose et al., 2006; Kleine-Kohlbrecher et al., 2010), and performed rescue experiments by re-expressing the inactive form of JMJD-1.2 (called JMJD-1.2_JmjCmut) in the *tm3713* background. While wild-type JMJD-1.2 could restore normal PVQ guidance, the mutated protein did not (Fig. 3B and Table S1), revealing the essential role of JMJD-1.2 catalytic activity in the process of axon guidance. Interestingly, mutations affecting the demethylase activity of the human homolog PHF8 are linked to neurological disorders (Koivisto et al., 2007; Loenarz et al., 2010; Qiu et al., 2010). Among others, the missense mutation c.836C>T encodes a F279S variant of the protein that is associated with mild XLMR and dysmorphic features (Koivisto et al., 2007). This mutation resides in the JmjC domain and has been shown to disrupt the catalytic activity of the protein (Loenarz et al., 2010; Qiu et al., 2010). As the region is highly conserved in *C. elegans*, we could generate a version of JMJD-1.2 bearing a similar mutation (called JMJD-1.2_XLMR, Fig. 3A). When re-expressed in the *tm3713* background, this mutant protein did not rescue PVQ axon guidance defects (Fig. 3B and Table S1).

Besides the JmjC domain, JMJD-1.2 carries a PHD finger that, like in the mammalian counterpart, has been shown to mediate the binding to H3K4me3 and to contribute to the demethylase activity, both *in vitro* and *in vivo* (Lin et al., 2010). To assess the role of this domain in the process of axon guidance, we generated a mutation in a specific residue that is important for the binding to H3K4me3 and for the catalytic activity of JMJD-1.2 (Lin et al., 2010; Yang et al., 2010). Like the catalytic-inactive protein, the enzyme bearing a mutated PHD finger (called JMJD-1.2_PHDmut, Fig. 3A) was unable to restore correct axon guidance (Fig. 3B and Table S1). All together, these data show that the JmjC domain and the PHD finger are both required for correctly driving the process of axon guidance and indicate that the demethylase activity and the binding ability of JMJD-1.2 to H3K4me3 are essential in this context.

jmjd-1.2 defects depend on deregulated transcription

Previously, it has been reported that loss of JMJD-1.2 is associated with deregulated gene transcription (Lin et al., 2010). As the activity of *jmjd-1.2* is important during embryogenesis, we analyzed the transcriptome of *jmjd-1.2(tm3713)* mutant embryos by RNA-sequencing. Notably, only 22 genes displayed expression changes of more than 1.5-fold between wild-type and mutants, of which 16 could be further validated by qPCR (Table 2). All validated genes are significantly upregulated in this allele (Table 2 and Fig. S4). We speculated that, if the overexpression of these genes was responsible for *jmjd-1.2* axon guidance defects, their removal from the *tm3713* background could ameliorate the axonal phenotype. As viable mutants for some of these genes are available, we generated double mutants with *jmjd-1.2* that we analyzed for PVQ defects. Loss of either *clec-230*, *cut-3*, *wrt-8* or *grl-16* could restore correct PVQ guidance (Fig. 4A and Table S2). Interestingly, both *wrt-8* and *grl-16* encode Hedgehog-related proteins (Aspöck et al., 1999; Hao et al., 2006b), raising the possibility that *C. elegans* Hedgehog signaling, similarly to the vertebrate counterpart, might play a key role in axon guidance. To strengthen this hypothesis, we tested whether overexpression of *wrt*-8 or *grl-16* in wild-type embryos could reproduce the PVQ guidance defects observed in *jmjd-1.2* mutants. As we were unable to obtain transgenic lines continuously overexpressing these proteins, we generated animals that carry heat-shock inducible *wrt-8* or *grl-16* genomic regions, using the *hsp-16.2* promoter. Strikingly, when *wrt-8* or *grl-16* expression was transiently induced during embryogenesis, we observed PVQ axon defects that were similar to the ones associated with loss of JMJD-1.2, both qualitatively and quantitatively (Fig. 4B-D). Importantly, this effect was not observed when the expression was forced at later developmental stages, as for example in L1, providing an important internal control and supporting the role of *jmjd-1.2* in regulating the expression of *wrt-8* or *grl-16* in embryos.

jmjd-1.2 axonal defects depend on Hedgehog signaling

Although in *C. elegans* the Hedgehog pathway has undergone a prominent divergence during evolution, some key molecules of the canonical Hedgehog signaling are conserved (Bürglin and Kuwabara, 2006; Kolotuev et al., 2009) (Table S3) and involved in trafficking of proteins and sterols, similarly to the vertebrate counterparts (Kuwabara et al., 2000; Hao et al., 2006b; Soloviev et al., 2011). As the defects observed in *jmjd-1.2* mutants are related to increased level of Hedgehog-related genes, we speculated that a negative regulation of the Hedgehog pathway could ameliorate the *jmjd-1.2* phenotype. Homologs of genes required for Hedgehog release (*DISP*/*che-14*) and propagation of the signal (*Glypican-6/gpn-1, EXT1/rib-1* or

EXTL3/rib-2) have been identified in *C. elegans*. We analyzed the effect of reduction (by RNA interference) or depletion (using mutants when available) of these conserved genes in *jmjd-1.2* background and invariantly observed a significant decrease of the *jmjd-1.2* axon guidance phenotype (Table 3). Similarly, we predicted that reduction of Hedgehog-like receptors and co-receptors (Patched/PTC-1/PTC-3, Megalin/LRP2/LRP-1, Gas1/PHG-1) could also influence the *jmjd-1.2* phenotype. Strikingly, reduction of *lrp-1*, *phg-1* and *ptc-1*, but not *ptc-3*, in *jmjd-1.2* mutants also resulted in significant amelioration of the phenotype, further supporting a causal role of deregulated Hedgehog signaling in the defective axon guidance of the *jmjd-1.2* mutant (Table 3). Instead, reduction of homologs of *skn*/*hhat-1/hhat-2*, required for palmitoylation of Hedgehog ligands, failed to significantly ameliorate the phenotype, similarly to the ablation of *grl-7*, another Hedgehog-related protein found upregulated in our RNA-sequencing data. Overall, the genetic ablation or reduction by RNAi of several conserved components of the Hedgehog pathway from the *tm3713* background is sufficient to rescue the PVQ defects associated with loss of *jmjd-1.2*. The evidence that the defects observed in *jmjd-1.2* mutant can be rescued by its ectopic expression in hypodermis or neurons suggests that the components of the Hedgehog pathway might be deregulated in multiple tissues and that the re-expression of *jmjd-1.2* in hypodermis or neuron is sufficient to restore a correct level of Hedgehog signaling and therefore a proper axon guidance.

All together, these findings strongly suggest that aberrant activation of Hedgehog signaling is responsible for the defects observed in *jmjd-1.2* mutants. Furthermore, our data provide the first evidence that some evolutionarily conserved proteins of the Hedgehog signaling act in axon guidance in *C. elegans*.

Implication of actin dynamics in *jmjd-1.2* defects

Many studies in several model organisms, including *C. elegans*, indicate that axon growth and guidance are ultimately regulated by actin cytoskeleton remodeling at growth cones (Kalil and Dent, 2005; Quinn and Wadsworth, 2008; Dent et al., 2011; Chia et al., 2014; Gomez and Letourneau, 2014). We therefore postulated that *jmjd-1.2* may regulate actin dynamics and tested this possibility by systematically ablating several conserved actin regulators in the *jmjd-1.2* genetic background and further analyzing the axon migration of PVQ neurons. We generated double mutants carrying the *jmjd-1.2* deletion together with mutations in well-established actin-regulator genes such as *wsp-1*/WASP, *wve-1*/WAVE, *unc-34*/Ena/VASP, *cdc-42*/CDC42, *mig-2*/RAC, *nck-1*/NCK and *wip-1*/WIP. While the removal of *wve-1*, *mig-2*, *unc-34*, *cdc-42* was ineffective, loss of *wsp-1* and its regulators *wip-1* and *nck-1* resulted in a

significant rescue of the *jmjd-1.2* phenotype (Fig. 4E), strongly suggesting that the *jmjd-1.2* axonal defects depend on aberrant actin remodeling mediated by *wsp-1*. Of note, none of the actin regulators are apparently deregulated at the transcriptional level in *jmjd-1.2* mutant animals, as indicated by RNA sequencing analysis, suggesting that Hh signaling in *C. elegans* may regulate axon migration in a transcriptional-independent manner. Importantly, overexpression of *grl-16* or *wrt-8* in a *wsp-1* background was unable to induce PVQ axon guidance defects, suggesting that the axonal defects observed in *jmjd-1.2* mutant depend on Hedgehog-mediated actin regulation (Fig. 4F). This hypothesis is in agreement with previous studies reporting that Hedgehog triggers a transcription-independent signaling cascade acting rapidly and locally at the growth cone to regulate actin-based structures dynamics and axon migration (Charron and Tessier-Lavigne, 2005; Bijlsma et al., 2007; Yam et al., 2009; Sasaki et al., 2010). All together these experiments suggest that *jmjd-1.2* regulates Hedgehog signaling and actin reorganization at the growth cone of migrating neurons.

DISCUSSION

In this study, we have found that *jmjd-1.2* regulates some aspects of neuronal development, including axon guidance (PVQs and HSNs) and neuronal cell body migration (HSNs). As the axon migration in PVQs and HSNs occurs during embryonic and larval stages, respectively, these results suggest a regulatory role for *jmjd-1.2* across development. We have also observed reduced expression of the terminal selector gene *unc-129* in the DB5 motoneuron, supporting a function of *jmjd-1.2* in the process of neuronal differentiation. Interestingly, this deficiency might contribute to the locomotion defects previously described in *jmjd-1.2* mutants (Kleine-Kohlbrecher et al., 2010).

Notably, the catalytic activity of JMJD-1.2 is fundamental to ensure correct axon guidance. Given that this demethylase is able to remove the dimethyl mark from different lysine residues on H3, we cannot, at the moment, link the observed neuronal defects to a specific activity of *jmjd-1.2* on one or more residues. In addition, our results indicate that the correct recruitment of JMJD-1.2 to chromatin, mediated by the PHD domain, is similarly important. It has been previously shown that JMJD-1.2 and its mammalian homolog PHF8 are recruited at promoters, where they control gene expression (Lin et al., 2010; Kleine-Kohlbrecher et al., 2010; Fortschegger et al., 2010). By RNA-sequencing, we identified minor changes in the transcriptome of *jmjd-1.2* mutant embryos compared to wild-type, and the few perturbed genes

were upregulated. While the low number of deregulated genes detected could be related to the experimental setting (we used mixed populations of embryos, which could have hidden tissue- and stage-specific changes in gene expression), the upregulation of gene transcription in association with increased levels of H3K9/K27/K23me2, marks that have been generally linked to gene repression, is unexpected and suggests that the deregulated genes may be indirect targets of JMJD-1.2.

Among the upregulated genes, we identified two encoding the Hedgehog-related proteins WRT-8 and GRL-16, and showed that their transient over-expression in wild-type embryos induces axon guidance defects similar to the ones identified in *jmjd-1.2* mutant animals. This observation strongly suggests that deregulation of *wrt-8* and *grl-16* is causal for the *jmjd-1.2* axonal phenotype. Further, we have shown that loss or reduction of genes encoding homologs of components of the Hedgehog pathway, including *wrt-8* and *grl-16*, is sufficient to rescue the *jmjd-1.2* defects. These results support a previously unappreciated role of Hedgehog-like signaling in *C. elegans* axon guidance. Two other genes were found upregulated in *jmjd-1.2* mutant animals, and their loss was sufficient to restore normal axon guidance in *jmjd-1.2* mutants: *clec-230* encodes a protein of 179 amino acids containing a lectin domain, a carbohydrate-binding module often found in proteins with functions in adhesion (Drickamer and Dodd, 1999), while *cut-3* encodes a component of the worm cuticle, specifically expressed in embryo (Sapio et al., 2005). Neither *cut-3* or *clec-230* has clear homologs in mammals and they were not further investigated. While it is possible that these genes are Hh transcriptional target genes, it is also conceivable that, being molecules implicated in adhesion and extracellular matrix composition, they could play a role in Hedgehog diffusion.

The role of the Hedgehog pathway in axon guidance is still poorly understood, but some studies indicate that in this context Hedgehog triggers an alternative, transcription-independent, signaling cascade acting rapidly and locally at the growth cone to induce actin cytoskeleton remodeling (Charron and Tessier-Lavigne, 2005; Bijlsma et al., 2007; Yam et al., 2009; Sasaki et al., 2010). Interestingly, our genetic interaction analyses suggest that molecules regulating actin dynamics play a role in the establishment of the aberrant *jmjd-1.2* axonal migration. In support of this finding, it has been previously reported that downregulation of PHF8 results in cytoskeleton disorganization and in cell adhesion defects (Asensio-Juan et al., 2012). It is possible that altered actin dynamics counteract the effects of increased Hedgehog signaling by regulating Hh trafficking and secretion. However, based on our previous findings that misexpression of actin regulators in PVQ neurons causes aberrant axon guidance (Mariani et al., 2016) and on our overexpression experiments in *wsp-1* genetic background, we favor the

hypothesis, presented in Fig. 5, in which JMJD-1.2 modulates the expression of Hedgehog-related proteins in neuronal and hypodermal cells, which, after secretion, activate a signaling pathway controlling actin remodeling and axon guidance in target neurons. How deregulation of the Hedgehog pathway impacts actin dynamics thereby leading to incorrect axon guidance is a key aspect that remains to be investigated. As we did not identify any transcriptional deregulation of actin regulators in *jmjd-1.2* mutants by RNA-sequencing, it is tempting to speculate that JMJD-1.2 might modulate the activity and/or cellular localization of actin regulators. Similarly, the tissue specificity of Hedgehog signaling components remains unknown and further analyses will be required to identify not only the specific cells secreting the ligands (signaling cells) but also the ones expressing Hedgehog receptors (receiving cells). Theoretically, despite obtained in *C. elegans*, our results suggest that aberrant Hedgehog pathway could be related to XLMR and other cognitive diseases, like intellectual disability (ID) or autism spectrum disorder (ASD). Supporting this possibility, the Hedgehog acyltransferase HHAT has been identified as mutated in whole-exon sequencing and proposed as a candidate gene for ID (Agha et al., 2014). Similarly, PTCHD1, which shares high homology with the Patched receptors, has been suggested as a candidate gene for ASD and ID (Noor et al., 2010; Filges et al., 2011; Chaudhry et al., 2015).

We recently identified RBR-2, an H3K4me3/2 histone demethylase, as also implicated in the regulation of axon guidance. *rbr-2* is the sole nematode homolog of the human XLMR gene *JARID1C*, and controls axon guidance in a similar subset of neurons by reducing the expression of actin-related genes, including *wsp-1* (Mariani et al., 2016). The fact that *rbr-2* and *jmjd-1.2* share similar phenotypes when ablated, are both required during embryogenesis and bind H3K4me3 through their PHD domains suggests that these histone demethylases may regulate axon guidance in a concerted manner. Indeed, we previously reported that *rbr-2;jmjd-1.2* double mutant showed similar levels of PVQ defects when compared to single mutants (Mariani et al., 2016), confirming that *rbr-2* and *jmjd-1.2* act in a common pathway regulating axon guidance. All together, these findings confirm that epigenetic factors are essential for the correct execution of developmental processes, providing novel insights into how neuronal development is achieved.

In conclusion, our study reveals a novel function of *jmjd-1.2* in axon guidance and provides the first evidence that the Hedgehog-like pathway conserved in *C. elegans* contributes to the correct establishment of axon migration.

MATERIALS AND METHODS

Genetics and strains

C. elegans strains were cultured using standard growth conditions at 20°C on *Escherichia coli* OP50 (Brenner, 1974). Strains were used as follows: wild-type Bristol: N2; *jmjd-1.2(tm3713)* IV; CX5334: *oyIs14[(Psra-6::GFP) + lin-15(+)]* V; MU1085: *bwIs2[(Pflp-1::GFP) + (pRF4)rol-6(su1006)]*; OH4887: *otIs182[Pinx-18::GFP]*; VH648: *hdIs26(Podr-2::CFP; Psra-6::DsRed2)* III; SK4013: *zdIs13[Ptph-1::GFP]* IV; EG1285: *oxIs12[(Punc-47::GFP) + lin-15(+)]* X; NW1100: *evIs82b[(Punc-129::GFP) + dpy-20(+)]* IV; LE309: *lqIs2 [Posm-6::GFP + lin-15(+)]* X; *wrt-8(tm1585)* V; RB2308: *C29F3.5/clec-230(ok3131)* V; *asp-6(tm2213)* V; RB1999: *grl-7(ok2644)* V; RB2183: *grl-16(ok2959)* I; VC2627: *F54F11.2/nep-17(ok3251)* III; VC1333: *evl-20&cut-3(ok1819)/mIn1[mIs14 dpy-20(e128)]* II; VC233: *gpn-1(ok377)* X; CB3687: *che-14(e1960)* I; ML514: *che-14(ok193)* I; *wsp-1(gm324)* IV; VC2053: *wip-1(ok2435)* III*/hT2 [bli-4(e937); let-?(q782); qIs48]* (I;III); VC898: *cdc-42(gk388)/mIn1 [mIs14*; *dpy-10(e128)]* II; RB860: *nck-1(ok694)* X; CF162: *mig-2(mu28)* X; VC2706: *wve-1(ok3308)* I*/hT2 [bli-4(e937); let-?(q782); qIs48]* (I;III); CB566: *unc-34(e566)* V. Double mutant animals were generated by standard crossing procedure. For a complete list of the transgenic strains generated for this study, see Table S4.

Generation of *jmjd-1.2(KO)* by CRISPR/Cas9

We generated a null mutant for *jmjd-1.2* [here called *jmjd-1.2(KO)*] by the co-CRISPR approach described in Ward et al., 2015. To identify the deletions, the following oligonucleotides were used: jmjd-1.2Fw (ATGCTGCGTCTCGTTTCTCT), jmjd-1.2Rev1 (TCATGTCGCTCATTTCAAGC), jmjd-1.2Rev2 (ACATCGATCCGATTCCTTTG). The resulting PCR products were purified and sequenced. The mutation used in this study consists of a deletion of 4,019 bp, starting 5 nucleotides upstream the *jmjd-1.2* ATG (IV:4660991) and ending 82 nucleotides after the stop codon. Sequences of sgRNAs are reported below.

sgRNA1_Fw: 5´ TCTTGATCTACACATTCCAAATGGA 3´

sgRNA1_Rev: 5´ AAACTCCATTTGGAATGTGTAGATC 3´

sgRNA2_Fw: 5´ TCTTGAAATTACTATTAAGATCGG 3´

sgRNA2_Rev: 5´ AAACCCGATCTTAATAGTAATTTC 3´

The *jmjd-1.2(KO)* allele was used to generate Fig. S1B.

Generation of transgenic constructs

The *jmjd-1.2::GFP* construct, a 4,715-bp fragment containing 786 bp of promoter and the entire genetic locus of *jmjd-1.2*, has been described previously (Kleine-Kohlbrecher et al., 2010). Plasmids carrying the *jmjd-1.2* gene fused to GFP and under specific promoters were constructed using MultiSite Gateway Three-Fragment Vector Construction Kit (Life Technologies).

The constructs used in Figs. 3B and 4B-D, F were generated as described in Supplementary Materials and Methods.

The DNA sequences of all constructs were verified by sequencing.

Microinjection and production of transgenic lines

Transgenic lines were obtained through microinjection (Mello et al., 1991). Constructs were injected into young adult hermaphrodites as extra-chromosomal arrays at 10-50 ng μl^{-1} with *Pttx-3::RFP* (50-90 ng μl^{-1}) or *Pmyo-2::mCherry* (0.5-5 ng μl^{-1}) as injection markers.

Fluorescence microscopy

For all transgenic markers, neuronal phenotypes were scored in L4 and young adult hermaphrodites grown at 25°C. Images were taken using an automated fluorescence microscope (Zeiss, AXIO Imager M2) and MicroManager software (version 1.4.11). All pictures were exported using Photoshop (Adobe).

Dil staining of amphid and phasmid neurons

Staining was performed as described previously (Mariani et al., 2016).

Heat-shock experiments

For overexpression experiments, embryos or L1 larvae were heat-shocked at 37°C two times for 30 minutes. After heat-shock, worms were kept at 25°C overnight and L2/L3 larvae were analyzed by fluorescence microscopy the day after.

RNAi analysis

RNA interference (RNAi) was performed by feeding and carried out as described previously (Timmons et al., 2001). Constructs were obtained from the *C. elegans* RNAi feeding library (J. Ahringer's laboratory, Wellcome Trust/Cancer Research UK Gurdon Institute, University of Cambridge, Cambridge, UK) except for *ptc-1*, *ptc-3*, *tra-1* and *phg-1*, which were cloned

into pCR2.1 TOPO vector using TOPO TA Cloning Kit (Life Technologies). Empty L4440 vector was used as negative control. F2 progeny was analyzed for axon guidance defects at L4 stage. Three individual plates were scored for each variable, in three biological independent experiments. We observed a decreased percentage of defects in *jmjd-1.2(tm3713)* and wild-type animals treated with L4440 compared to *jmjd-1.2(tm3713)* mutants (Table 3), suggesting that the phenotype measured is, for unclear reasons, sensitive to the bacterial strain used as source of food. However, *jmjd-1.2(tm3713)* mutants treated with L4440 have still a significant increased percentage of defects when compared to wild-type animals grown on similar conditions (p = 0.0002).

RNA-sequencing

Gravid hermaphrodites cultured at 25°C were treated with hypochlorite solution and embryos were flash-frozen in liquid nitrogen and stored at -80°C before RNA extraction. RNA was isolated from two independent cultures using TRIzol reagent (Life Technologies) and RNeasy Minikit (Qiagen). RNA amplification and sequencing were performed by the Beijing Genomics Institute (BGI).

RNA-sequencing analysis

Bar code and adaptor-cleaned sequences were checked for quality using FastQC and mapped to *C. elegans* genome (WS220) with TopHat 2.0.9 (Trapnell et al., 2012), using parameters as described previously (Peltonen et al., 2013). Reads successfully mapped were >95% using a criteria of two mismatches. The number of reads processed and % aligned were: wild-type replicate 1, 43.2 M, 95.8%; wild-type replicate 2, 37.8 M, 96.0%; *jmjd-1.2* replicate 1, 39.9 M, 95.8%; *jmjd-1.2* replicate 2, 34.7 M, 95.9%. Mapped reads were analyzed for transcript assembly and differential expression, using Cufflinks 2.1.1 with a filter of 1.5-fold difference and FDR correction (p value<0.05). Differentially expressed genes were used for gene set enrichment analysis (GSEA) performed using DAVID 6.7 (Huang da et al., 2009). Data were submitted to NCBI SRA public database with the following accession numbers: BioProject, PRJNA354814; BioSample, SAMN06052359; Data, SRR5051663, SRR5051664, SRR5051665, SRR505165.

Real-time quantitative PCR (RT–qPCR)

RNA isolation, cDNA synthesis and qPCR were performed as described previously (Mariani et al., 2016). The measures were normalized to *Y45F10D.4* (Zhang et al., 2012). All reactions were performed in duplicate, in two independent experiments.

Generation of antibody against JMJD-1.2

A polyclonal antibody against JMJD-1.2 was generated by Innovagen AB (IDEON Gamma Rec. Solvegatan 41 SE-22362 Lund, Sweden), by immunizing rabbits with a purified bacterial GST-tagged fragment of the JMJD-1.2 protein encoded by the first four exons of the gene. The antibody was affinity purified.

Western blot analysis

Whole-worm lysates for SDS-PAGE were prepared by boiling mixed stage worms in SDS-PAGE loading buffer for 5 minutes. Protein concentration was estimated using the modified micro-Lowry assay. The following antibodies were used: rabbit polyclonal anti-JMJD-1.2 (Innovagen AB1) 1:1,000; mouse monoclonal anti-actin (Millipore) 1:15,000; peroxidase-labeled anti-rabbit and anti-mouse secondary antibodies (Vector) 1:10,000.

Immunofluorescence

Whole worms were stained according to Finney and Ruvkun, 1990. Primary antibody [polyclonal anti-JMJD-1.2 (Innovagen AB1)] was incubated overnight at 4°C in a humid chamber and secondary antibody [goat anti-rabbit IgG (Alexafluor 594, Invitrogen)] was incubated 1 hour at room temperature. Washes were in PBS/Tween 0.2%. Vectashield H1200 mounting medium for fluorescence with DAPI was used to counterstain DNA.

Statistical analyses

All phenotypes were scored as percentages of defective animals. Statistical analyses were performed in GraphPad Prism 6 using Fisher's exact test, for pairwise comparisons, or one-way ANOVA followed by Tukey's multiple-comparison test, for multiple comparisons. In rescue and overexpression experiments, significance was calculated in relation to non-transgenic controls for each transgenic line. As the penetrance of defects in non-transgenic siblings was always consistent with the phenotype of *jmjd-1.2(tm3713)*, these data are not shown in Figs 2B, 2C, 3B and S3C. qPCR data are compared using Student's *t-test*. Differences with a p value <0.05 were considered significant.

ACKNOWLEDGEMENTS

Some strains were provided by the CGC, which is funded by NIH Office of Research Infrastructure Programs (P40 OD010440). We thank the National BioResource project for *C. elegans* (Japan) and the international *C. elegans* Gene Knockout Consortium for providing strains; the Beijing Genomics Institute (BGI) for performing the RNA amplification and sequencing; Innovagen AB for generating the antibody against JMJD-1.2. We are grateful to Roger Pocock for strains and discussion and to Alexandra Avram, Andreea Talos and Line Kikarsen for technical assistance.

COMPETING INTERESTS

No competing interests declared.

AUTHOR CONTRIBUTIONS

A.R., L.M. E.M. and P.G.A. carried out all the experimental work. J.P. and G.W. analyzed the RNA-sequencing data. A.R., L.M., E.M., P.G.A. and A.E.S designed the experiments and analyzed the data. L.M. and A.E.S. wrote the manuscript.

FUNDING

This work was supported by the Danish National Research Foundation (DNRF82 to A.E.S.) and University of Macau research grant (MYRG2015-00231-FHS to G.W.).

REFERENCES

Abidi, F., Miano, M., Murray, J. and Schwartz, C. (2007). A novel mutation in the *PHF8* gene is associated with X-linked mental retardation with cleft lip/cleft palate. *Clin. Genet.*, **72**, 19-22.

Agha, Z., Iqbal, Z., Azam, M., Ayub, H., Vissers, L. E., Gilissen, C., Ali, S. H., Riaz, M., Veltman, J. A., Pfundt, R., *et al.* (2014). Exome sequencing identifies three novel candidate genes implicated in intellectual disability. *PLoS One*, **9**, e112687.

Asensio-Juan, E., Gallego, C. and Martínez-Balbás, M. A. (2012). The histone demethylase PHF8 is essential for cytoskeleton dynamics. *Nucleic Acids Res.*, **40**, 9429-40.

Aspöck, G., Kagoshima, H., Niklaus, G., Bürglin, T.R. (1999). *Caenorhabditis elegans* has scores of Hedgehog-related genes: sequence and expression analysis. *Genome Res.*, **10**, 909-23.

Aurelio, O., Hall, D. H. and Hobert, O. (2002). Immunoglobulin-domain proteins required for maintenance of ventral nerve cord organization. *Science*, **295**, 686-90.

Ayala, R., Shu, T. and Tsai, L. H. (2007). Trekking across the brain: the journey of neuronal migration. *Cell*, **128**, 29-43.

Bénard, C. Y., Blanchette, C., Recio, J. and Hobert, O. (2012). The secreted immunoglobulin domain proteins ZIG-5 and ZIG-8 cooperate with L1CAM/SAX-7 to maintain nervous system integrity. *PLoS Genet.*, **8**, e1002819.

Bijlsma, M. F., Borensztajn, K. S., Roelink, H., Peppelenbosch, M. P. and Spek, C. A. (2007). Sonic hedgehog induces transcription-independent cytoskeletal rearrangement and migration regulated by arachidonate metabolites. *Cell Signal.*, **19**, 2596-604.

Bourikas, D., Pekarik, V., Baeriswyl, T., Grunditz, A., Sadhu, R., Nardo, M. and Stoeckli, E. T. (2005). Sonic hedgehog guides commissural axons along the longitudinal axis of the spinal cord. *Nat. Neurosci.*, **8**, 297-304.

Brenner, S. (1974). The genetics of *Caenorhabditis elegans*. *Genetics*, **77**, 71-94.

Bürglin, T.R., and Kuwabara, P.E. (2006). Homologs of the Hh signalling network in *C. elegans*. WormBook: the online review of *C elegans* biology **28**, 1-14.

Charron, F. and Tessier-Lavigne, M. (2005). Novel brain wiring functions for classical morphogens: a role as graded positional cues in axon guidance. *Development*, **132**, 2251-62.

Chaudhry, A., Noor, A., Degagne, B., Baker, K., Bok, L. A., Brady, A. F., Chitayat, D., Chung, B. H., Cytrynbaum, C., Dyment, D., *et al.* (2015). Phenotypic spectrum associated with PTCHD1 deletions and truncating mutations includes intellectual disability and autism spectrum disorder. *Clin. Genet.*, **88**, 224-33.

Chia, P. H., Chen, B., Li, P., Rosen, M. K. and Shen, K. (2014). Local F-actin network links synapse formation and axon branching. *Cell*, **156**, 208-20.

Chiurazzi, P., Tabolacci, E. and Neri, G. (2004). X-linked mental retardation (XLMR): from clinical conditions to cloned genes. *Crit. Rev. Clin. Lab. Sci.*, **41**, 117-58.

Dent, E. W., Gupton, S. L. and Gertler, F. B. (2011). The growth cone cytoskeleton in axon outgrowth and guidance. *Cold Spring Harb. Perspect. Biol.*, **3**.

Drickamer, K. and Dodd, R. B. (1999). C-Type lectin-like domains in *Caenorhabditis elegans*: predictions from the complete genome sequence. *Glycobiology*, **9**, 1357-69.

Feng, W., Yonezawa, M., Ye, J., Jenuwein, T. and Grummt, I. (2010). PHF8 activates transcription of rRNA genes through H3K4me3 binding and H3K9me1/2 demethylation. *Nat. Struct. Mol. Biol.*, **17**, 445-50.

Filges, I., Rothlisberger, B., Blattner, A., Boesch, N., Demougin, P., Wenzel, F., Huber, A. R., Heinimann, K., Weber, P. and Miny, P. (2011). Deletion in Xp22.11: PTCHD1 is a candidate gene for X-linked intellectual disability with or without autism. *Clin. Genet.*, **79**, 79-85.

Finney, M. and Ruvkun, G. (1990). The *unc-86* gene product couples cell lineage and cell identity in *C. elegans*. *Cell.*, 63, 895-905.

Fortschegger, K. and Shiekhattar, R. (2011). Plant homeodomain fingers form a helping hand for transcription. *Epigenetics*, **6**, 4-8.

Fortschegger, K., De Graaf, P., Outchkourov, N. S., Van Schaik, F. M., Timmers, H. T. and Shiekhattar, R. (2010). PHF8 targets histone methylation and RNA polymerase II to activate transcription. *Mol. Cell. Biol.*, **30**, 3286-98.

Gomez, T. M. and Letourneau, P. C. (2014). Actin dynamics in growth cone motility and navigation. *J. Neurochem.*, **129**, 221-34.

Guerrero, I. and Kornberg, T. B. (2014). Hedgehog and its circuitous journey from producing to target cells. *Semin. Cell. Dev. Biol.*, **33**, 52-62.

Hammond, R., Blaess, S. and Abeliovich, A. (2009). Sonic hedgehog is a chemoattractant for midbrain dopaminergic axons. *PLoS One*, **4**, e7007.

Hao, L., Aspöck, G. and Bürglin, T. R. (2006a). The hedgehog-related gene *wrt-5* is essential for hypodermal development in *Caenorhabditis elegans*. *Dev. Biol.*, **290**, 323-36.

Hao, L., Johnsen, R., Lauter, G., Baillie, D. and Bürglin, T. R. (2006b). Comprehensive analysis of gene expression patterns of hedgehog-related genes. *BMC Genomics*, **7**, 280.

Huang, C., Xiang, Y., Wang, Y., Li, X., Xu, L., Zhu, Z., Zhang, T., Zhu, Q., Zhang, K., Jing, N., *et al.* (2010). Dual-specificity histone demethylase KIAA1718 (KDM7A) regulates neural differentiation through FGF4. *Cell Res.*, **20**, 154-65.

Huang da, W., Sherman, B. T. and Lempicki, R. A. (2009). Bioinformatics enrichment tools: paths toward the comprehensive functional analysis of large gene lists. *Nucleic Acids Res.*, **37**, 1-13.

Jarov, A., Williams, K. P., Ling, L. E., Koteliansky, V. E., Duband, J. L. and Fournier-Thibault, C. (2003). A dual role for Sonic hedgehog in regulating adhesion and differentiation of neuroepithelial cells. *Dev. Biol.*, **261**, 520-36.

Jenkins, D. (2009). Hedgehog signalling: emerging evidence for non-canonical pathways. *Cell Signal.*, **21**, 1023-34.

Kalil, K. and Dent, E. W. (2005). Touch and go: guidance cues signal to the growth cone cytoskeleton. *Curr. Opin. Neurobiol.*, **15**, 521-6.

Kleine-Kohlbrecher, D., Christensen, J., Vandamme, J., Abarrategui, I., Bak, M., Tommerup, N., Shi, X., Gozani, O., Rappsilber, J., Salcini, A. E. *et al.* (2010). A functional link between the histone demethylase PHF8 and the transcription factor ZNF711 in X-linked mental retardation. *Mol. Cell*, **38**, 165-78.

Klose, R. J., Kallin, E. M. and Zhang, Y. (2006). JmjC-domain-containing proteins and histone demethylation. *Nat. Rev. Genet.*, **7**, 715-27.

Koivisto, A. M., Ala-Mello, S., Lemmela, S., Komu, H. A., Rautio, J. and Jarvela, I. (2007). Screening of mutations in the PHF8 gene and identification of a novel mutation in a Finnish family with XLMR and cleft lip/cleft palate. *Clin. Genet.*, **72**, 145-9.

Kolotuev, I., Apaydin, A. and Labouesse, M. (2009). Secretion of Hedgehog-related peptides and WNT during *Caenorhabditis elegans* development. *Traffic*, **10**, 803-10.

Kuwabara, P.E., Lee, M.H., Schedl, T. and Jefferis, G.S. (2000). A *C. elegans* patched gene, *ptc-1*, functions in germ-line cytokinesis. *Genes Dev.* **14**, 1933-1944.

Laumonnier, F., Holbert, S., Ronce, N., Faravelli, F., Lenzner, S., Schwartz, C.E., Lespinasse, J., Van Esch, H., Lacombe, D., Goizet, C. *et al.* (2005). Mutations in PHF8 are

associated with X linked mental retardation and cleft lip/cleft palate. *J. Med. Genet.* **42**, 780-786.

Lin, H., Wang, Y., Wang, Y., Tian, F., Pu, P., Yu, Y., Mao, H., Yang, Y., Wang, P., Hu, L. *et al.* (2010). Coordinated regulation of active and repressive histone methylations by a dual-specificity histone demethylase ceKDM7A from *Caenorhabditis elegans*. *Cell Res.* **20**, 899-907.

Liu, W., Tanasa, B., Tyurina, O.V., Zhou, T.Y., Gassmann, R., Liu, W.T., Ohgi, K.A., Benner, C., Garcia-Bassets, I., Aggarwal, A.K. *et al.* (2010). PHF8 mediates histone H4 lysine 20 demethylation events involved in cell cycle progression. *Nature* **466**, 508-512.

Loenarz, C., Ge, W., Coleman, M.L., Rose, N.R., Cooper, C.D., Klose, R.J., Ratcliffe, P.J. and Schofield, C.J. (2010). PHF8, a gene associated with cleft lip/palate and mental retardation, encodes for an Nepsilon-dimethyl lysine demethylase. *Hum. Mol. Genet.* **19**, 217-222.

Mariani, L., Lussi, Y. C., Vandamme, J., Riveiro, A. and Salcini, A. E. (2016). The H3K4me3/2 histone demethylase RBR-2 controls axon guidance by repressing the actin-remodeling gene *wsp-1*. *Development*, **143**, 851-63.

Mello, C.C., Kramer, J.M., Stinchcomb, D. and Ambros, V. (1991). Efficient gene transfer in *C.elegans*: extrachromosomal maintenance and integration of transforming sequences. *EMBO J.* **10**, 3959-3970.

Noor, A., Whibley, A., Marshall, C.R., Gianakopoulos, P.J., Piton, A., Carson, A.R., Orlic-Milacic, M., Lionel, A.C., Sato, D., Pinto, D. *et al.* (2010). Disruption at the PTCHD1 Locus on Xp22.11 in Autism spectrum disorder and intellectual disability. *Sci. Transl. Med.* **2**, 49ra68.

Peltonen, J., Aarnio, V., Heikkinen, L., Lakso, M. and Wong, G. (2013). Chronic ethanol exposure increases cytochrome P-450 and decreases activated in blocked unfolded protein response gene family transcripts in *Caenorhabditis elegans*. *J. Biochem. Mol. Toxicol.* **27**, 219-228.

Pocock, R., Bénard, C.Y., Shapiro, L. and Hobert, O. (2008). Functional dissection of the *C. elegans* cell adhesion molecule SAX-7, a homologue of human L1. *Mol. Cell Neurosci.* **37**, 56-68.

Qi, H.H., Sarkissian, M., Hu, G.Q., Wang, Z., Bhattacharjee, A., Gordon, D.B., Gonzales, M., Lan, F., Ongusaha, P.P., Huarte, M. *et al.* (2010). Histone H4K20/H3K9 demethylase PHF8 regulates zebrafish brain and craniofacial development. *Nature* **466**, 503-507.

Qiu, J., Shi, G., Jia, Y., Li, J., Wu, M., Li, J., Dong, S. and Wong, J. (2010). The X-linked mental retardation gene PHF8 is a histone demethylase involved in neuronal differentiation. *Cell Res.* **20**, 908-918.

Quinn, C. C. & Wadsworth, W. G. (2008). Axon guidance: asymmetric signaling orients polarized outgrowth. *Trends Cell Biol.*, **18**, 597-603.

Redin, C., Gérard, B., Lauer, J., Herenger, Y., Muller, J., Quartier, A., Masurel-Paulet, A., Willems, M., Lesca, G., El-Chehadeh, S. *et al.* (2014). Efficient strategy for the molecular diagnosis of intellectual disability using targeted high-throughput sequencing. *J. Med. Genet.* **51**, 724-736.

Robichaux, M.A. and Cowan, C.W. (2014). Signaling mechanisms of axon guidance and early synaptogenesis. *Curr. Top. Behav. Neurosci.* **16**, 19-48.

Ropers, H.H. and Hamel, B.C. (2005). X-linked mental retardation. *Nat. Rev. Genet.* **6**, 46-57.

Sánchez-Camacho, C. and Bovolenta, P. (2008). Autonomous and non-autonomous Shh signalling mediate the in vivo growth and guidance of mouse retinal ganglion cell axons. *Development* **135**, 3531-3541.

Sapio, M.R., Hilliard, M.A., Cermola, M., Favre, R. and Bazzicalupo, P. (2005). The Zona Pellucida domain containing proteins, CUT-1, CUT-3 and CUT-5, play essential roles in the development of the larval alae in *Caenorhabditis elegans*. *Dev. Biol.* **282**, 231-245.

Sasaki, N., Kurisu, J. and Kengaku, M. (2010). Sonic Hedgehog signaling regulates actin cytoskeleton via Tiam1-Rac1 cascade during spine formation. *Mol. Cell. Neurosci.* **45**, 335-344.

Siderius, L.E., Hamel, B.C., van Bokhoven, H., de Jager, F., van den Helm, B., Kremer, H., Heineman-de Boer, J.A., Ropers, H.H. and Mariman, E.C. (1999). X-linked mental retardation associated with cleft lip/palate maps to Xp11.3-q21.3. *Am. J. Med. Genet.* **85**, 216-220.

Soloviev, A., Gallagher, J., Marnef, A. and Kuwabara, P.E. (2011). *C. elegans patched-3* is an essential gene implicated in osmoregulation and requiring an intact permease transporter domain. *Dev. Biol.* **351**, 242-253.

Sulston, J.E. (1983). Neuronal cell lineages in the nematode *Caenorhabditis elegans*. *Cold Spring Harb. Symp. Quant. Biol.* **48**, Pt 2:443-452.

Timmons, L., Court, D.L. and Fire, A. (2001). Ingestion of bacterially expressed dsRNAs can produce specific and potent genetic interference in *Caenorhabditis elegans*. *Gene* **263**, 103-112.

Trapnell, C., Roberts, A., Goff, L., Pertea, G., Kim, D., Kelley, D.R., Pimentel, H., Salzberg, S.L., Rinn, J.L. and Pachter, L. (2012). Differential gene and transcript expression analysis of RNA-seq experiments with TopHat and Cufflinks. *Nat. Protoc.* **7**, 562-578.

Tsukada, Y., Ishitani, T. and Nakayama, K. I. (2010). KDM7 is a dual demethylase for histone H3 Lys 9 and Lys 27 and functions in brain development. *Genes Dev.*, **24**, 432-7.

Vandamme, J., Sidoli, S., Mariani, L., Friis, C., Christensen, J., Helin, K., Jensen, O.N. and Salcini, A.E. (2015). H3K23me2 is a new heterochromatic mark in *Caenorhabditis elegans*. *Nucleic Acids Res.* **43**, 9694-9710.

Ward, J.D. (2015). Rapid and precise engineering of the *Caenorhabditis elegans* genome with lethal mutation co-conversion and inactivation of NHEJ repair. *Genetics*, **199**, 363-77.

Weinberg, P., Flames, N., Sawa, H., Garriga, G. and Hobert, O. (2013). The SWI/SNF chromatin remodeling complex selectively affects multiple aspects of serotonergic neuron differentiation. *Genetics*, **194**, 189-98.

White, J.G., Southgate, E., Thomson, J.N. and Brenner, S. (1986). The structure of the nervous system of the nematode *Caenorhabditis elegans*. *Philos. Trans. R. Soc. Lond. B Biol. Sci.* **314**, 1-340.

Yam, P.T. and Charron, F. (2013). Signaling mechanisms of non-conventional axon guidance cues: the Shh, BMP and Wnt morphogens. *Curr. Opin. Neurobiol.* **23**, 965-973.

Yam, P.T., Langlois, S.D., Morin, S. and Charron, F. (2009). Sonic Hedgehog guides axons through a noncanonical, Src-family-kinase-dependent signaling pathway. *Neuron* **62**, 349-362.

Yang, Y., Hu, L., Wang, P., Hou, H., Lin, Y., Liu, Y., Li, Z., Gong, R., Feng, X., Zhou, L. *et al.* (2010). Structural insights into a dual-specificity histone demethylase ceKDM7A from *Caenorhabditis elegans*. *Cell Res.* **20**, 886-898.

Zhang, Y., Chen, D., Smith, M.A., Zhang, B. and Pan, X. (2012). Selection of reliable reference genes in *Caenorhabditis elegans* for analysis of nanotoxicity. *PLoS One* **7**, e31849.

Zheng, C., Karimzadegan, S., Chiang, V. and Chalfie, M. (2013). Histone methylation restrains the expression of subtype-specific genes during terminal neuronal differentiation in *Caenorhabditis elegans*. *PLoS Genet.*, **9**, e1004017.

Zugasti, O., Rajan, J. and Kuwabara, P. E. (2005). The function and expansion of the Patched- and Hedgehog-related homologs in *C. elegans*. *Genome Res.*, **15**, 1402-10.

Table 1. Summary of phenotypes in *jmjd-1.2(tm3713)* mutants

	Defective animals (%)	
Neurons examined (*marker used*)	WT	*jmjd-1.2(tm3713)*
Head neurons		
Amphid neurons[a] (*DiI*)	0	0
Ventral cord neurons		
Interneurons		
AVK interneurons[b] (*bwIs2*)	0	3
AVG interneuron[b] (*otIs182*)	0	0
PVP interneurons[b] (*hdIs26*)	9	20 **
PVQ interneurons[b] (*oyIs14*)	9	22 ***
Motoneurons		
HSN motoneurons (*zdIs13*)		
axon guidance[b]	6	36 ***
cell migration[c]	5	34 ***
D-type motoneurons (*oxIs12*)		
midline left/right choice[d]	31	50
DA/DB motoneurons (*evIs82b*)		
midline left/right choice[d]	4	4
transgene expression reduced in DB5[e]	2	32 ***
DVB motoneuron[f] (*oxIs12*)	0	0
Sensory neurons		
PDE neurons[g] (*lqIs2*)	5	9
Tail neurons		
Phasmid neurons[a] (*DiI*)	0	0

Neurons examined using the indicated transgenic markers and the diffusible dye *DiI*. Statistical significance of the difference between wild-type and mutants was assessed with Fisher's exact test. $n > 100$, $^{**}p<0.01$, $^{***}p<0.001$. Animals were considered defective if: [a] neurons were not stained with a diffusible dye (*DiI*); [b] axons crossed over the VNC; [c] neuronal cells were misplaced; [d] the commissure of at least one motoneuron extended on the wrong side of the body; [e] transgene expression was reduced in DB5; [f] transgene expression was absent in DVB; [g] axons failed to reach the VNC.

Table 2. Genes with deregulated expression in *jmjd-1.2(tm3713)* mutants

Gene	Fold change	qPCR validation	Allele	Functions
C38D9.2	5.81	no	-	n.d.
wrt-8	4.08	yes	*tm1585*	Hh-like protein
F15E6.10	3.68	yes	-	n.d.
clec-230	3.13	yes	*ok3131*	C-type lectin
asp-6	2.05	yes	*tm2213*	Predicted protease
grl-7	2.05	yes	*ok2644*	Hh-like protein
C02E7.7	1.99	no	-	n.d.
C08B6.4	1.91	yes	-	Predicted chitinase activity
F10D11.6	1.90	yes	-	Predicted lipid binding
grl-16	1.89	yes	*ok2959*	Hh-like protein
asp-1	1.87	yes	-	Predicted protease
lgc-22	1.83	yes	-	Ligand-gated ion channel
ZK180.5	1.82	yes	-	n.d.
bcl-11	1.81	yes	-	Homology to BCL11A
Y47D7A.13	1.79	n.d.	-	n.d.
nep-17	1.77	yes	*ok3251*	Predicted metallopeptidase
cut-3	1.72	yes	*ok1819*	Cuticlin
F41F3.3	1.71	n.d.	-	n.d.
cut-2	1.62	yes	-	Cuticlin
drd-2	1.62	yes	-	Homology to TENM3
hsp-16.41	-2.0	no	-	Heat-shock protein
hsp-16.11	-2.2	no	-	Heat-shock protein

List of genes found deregulated by RNA-sequencing in *jmjd-1.2(tm3713)* compared to wild-type embryos. A filter of 1.5-fold difference and FDR correction ($p<0.05$) were applied. Validation by qPCR, available mutant alleles and the gene functions are indicated; n.d., not determined.

Table 3. Loss or reduction of distinct members of the Hedgehog family rescue PVQ defects in *jmjd-1.2(tm3713)* mutants

Genotype	Rescue	% defective animals	*n*	*p*-value
WT	-	9	> 400	-
jmjd-1.2(tm3713)	-	22	> 400	-
jmjd-1.2(tm3713);gpn-1(ok377)	yes	12	221	0.0186[a]
jmjd-1.2(tm3713);che-14(e1960)	yes	13	191	0.0269[a]
jmjd-1.2(tm3713);che-14(ok193)	yes	11	178	0.0023[a]
WT + *RNAi control*	-	5	346	-
jmjd-1.2(tm3713) + RNAi control	-	14	384	0.0002[c]
jmjd-1.2(tm3713) + lrp-1 RNAi	yes	8	474	0.0149[b]
jmjd-1.2(tm3713) + ptc-1 RNAi	yes	8	235	0.0334[b]
jmjd-1.2(tm3713) + ptc-3 RNAi	no	13	332	1.0000[b]
jmjd-1.2(tm3713) + rib-1 RNAi	yes	8	275	0.0344[b]
jmjd-1.2(tm3713) + rib-2 RNAi	yes	8	294	0.0496[b]
jmjd-1.2(tm3713) + hhat-1 RNAi	no	13	216	1.0000[b]
jmjd-1.2(tm3713) + hhat-2 RNAi	no	11	252	0.3467[b]
jmjd-1.2(tm3713) + tra-1 RNAi	no	16	504	0.2390[b]

[a]: compared to *jmjd-1.2(tm3713)*

[b]: compared to *jmjd-1.2(tm3713) + RNAi control*

[c]: compared to WT + *RNAi control*

Statistical significance was assessed with one-way ANOVA followed by Tukey's multiple-comparison test (*p* values are indicated). *n* = number of analyzed animals.

Figures

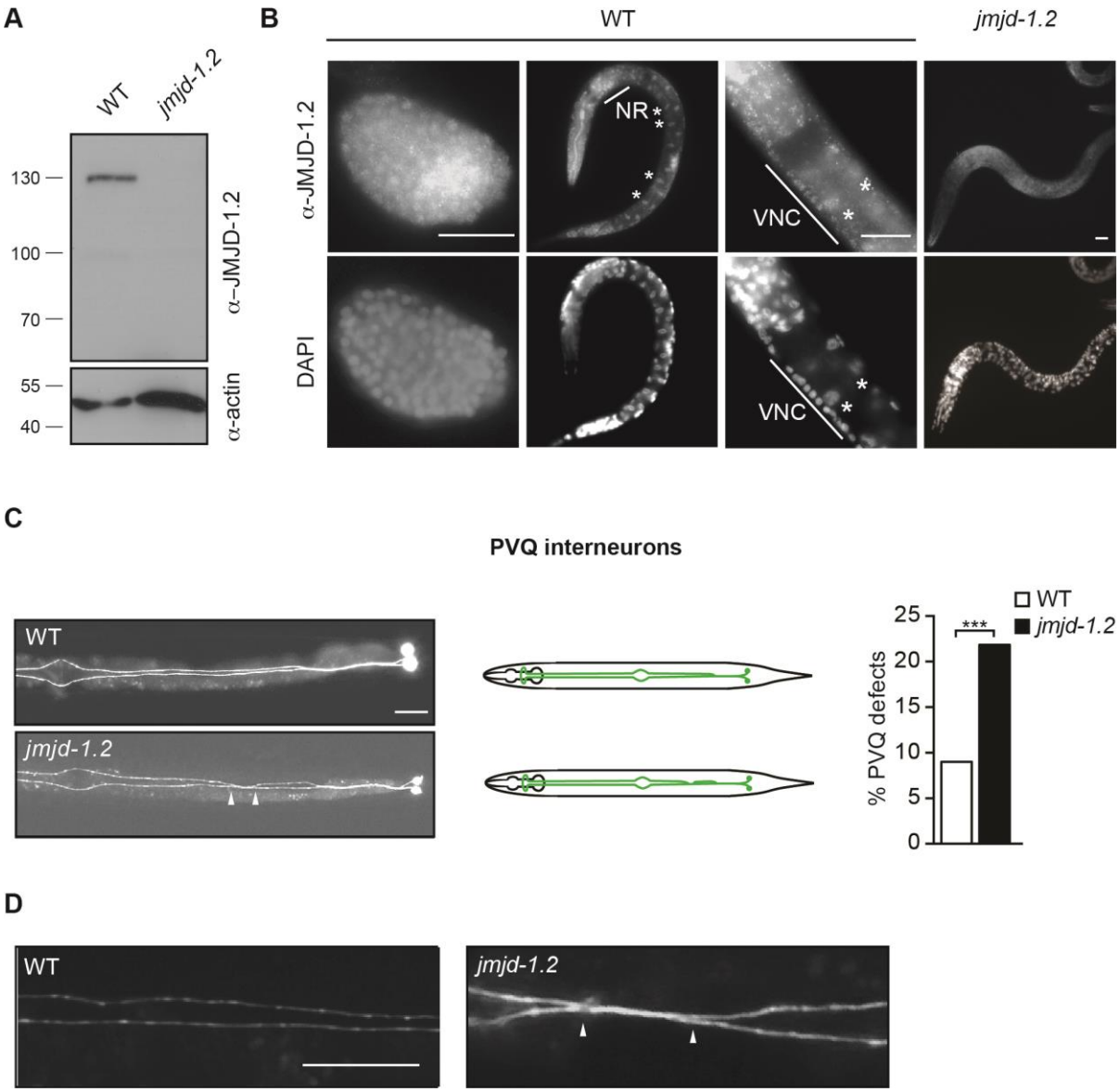

Fig. 1. JMJD-1.2 is required for correct axon guidance. A. Wild-type (WT) and *jmjd-1.2(tm3713)* whole-worm lysates assayed by immunoblotting with JMJD-1.2 antibody. Actin is used as loading control. **B.** Representative images of wild-type and *jmjd-1.2(tm3713)* animals, fixed and stained with JMJD-1.2 antibody. DNA was counterstained with DAPI. Asterisks indicate intestinal cells and the lines indicate neurons of the nerve ring (NR) or ventral nerve cord (VNC). **C.** Left: Representative images of PVQ neurons in wild-type and *jmjd-1.2(tm3713)* adult animals, visualized using the transgene *oyIs14*. Center: Schematic diagrams of PVQ neurons in wild-type and *jmjd-1.2(tm3713)* animals. Right: Quantification of

PVQ axonal cross-over defects in *jmjd-1.2(tm3713)* animals. $n > 200$, ***$p<0.001$ (Fisher's exact test). **D.** Large-sized image of PVQ axons in wild-type and *jmjd-1.2(tm3713)* adult animals, visualized using the transgene *oyIs14*. In (C) and (D), arrowheads indicate the points of axonal cross-over. Ventral view, anterior to the left. Scale bars, 20 μm.

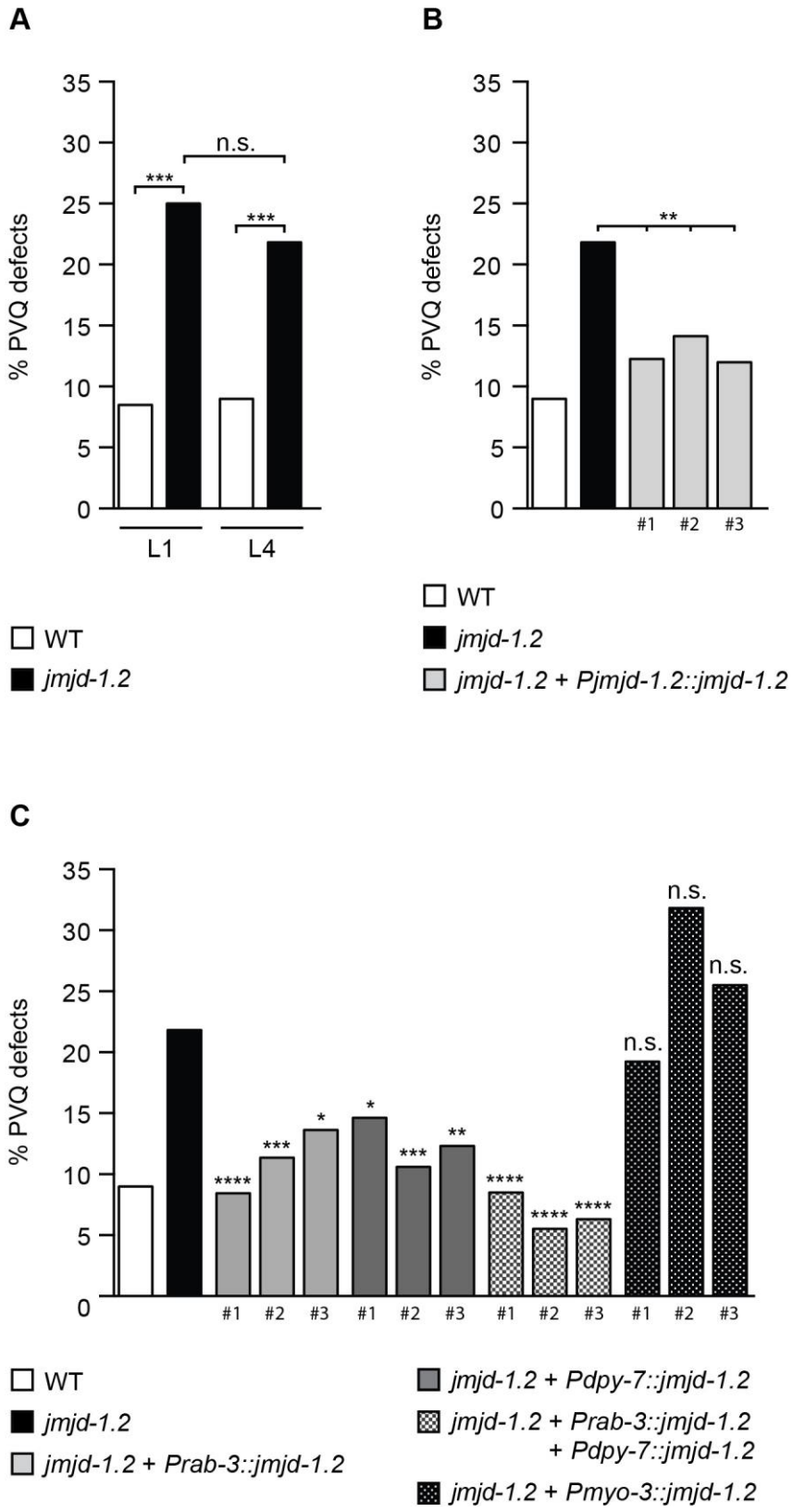

Fig. 2. JMJD-1.2 acts during embryogenesis in both nervous system and hypodermis to ensure correct axon guidance. A. Quantification of PVQ axonal cross-over defects in *jmjd-1.2(tm3713)* mutants at L1 and L4 stages. $n > 100$. **B.** Rescue of PVQ axonal cross-over defects in *jmjd-1.2(tm3713)* expressing the *Pjmjd-1.2::jmjd-1.2::GFP* translational reporter. **C.**

Tissue-specific rescue analyses. Promoters used for transgenic rescue are: *Prab-3*, nervous system; *Pdpy-7*, hypodermis; *Pmyo*-3, muscle cells. In (B) and (C), statistical significance was calculated in relation to non-transgenic controls (values not shown) for each transgenic line. $n > 100$. In all graphs, *$p<0.05$, **$p<0.01$, ***$p<0.001$, ****$p<0.0001$, n.s., not significant (one-way ANOVA followed by Tukey's multiple-comparison test). Three independent lines for each transgene (indicated by #) were analyzed.

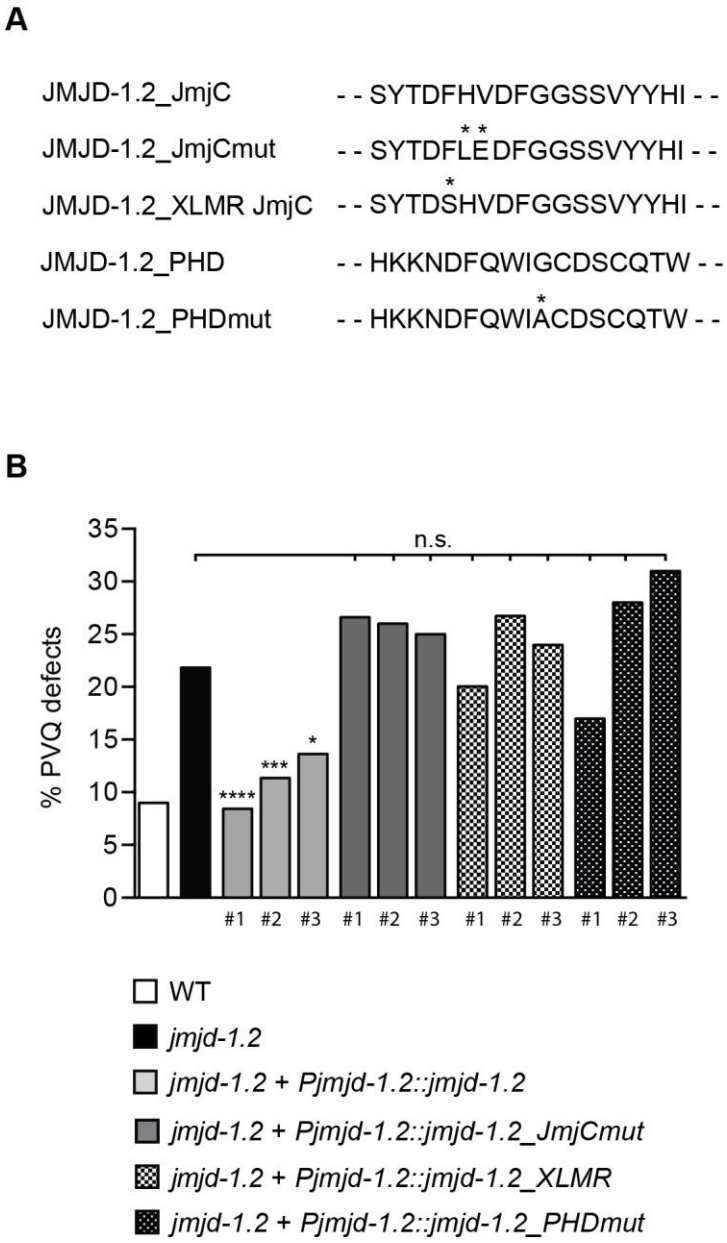

Fig. 3. The JmjC and the PHD finger domains of JMJD-1.2 are required for correct axon guidance. A. Parts of the JmjC and PHD finger domains of wild-type JMJD-1.2. Marked by asterisks, the amino acids mutagenized to generate the catalytically inactive JMJD-1.2 (JMJD-1.2_JmjCmut), the JMJD-1.2 bearing a mutation associated with X-linked mental retardation (JMJD-1.2_XLMR) and the JMJD-1.2 with mutated PHD finger (JMJD-1.2_PHDmut) constructs. **B.** Quantification of PVQ axonal cross-over defects in *jmjd-1.2(tm3713)* animals expressing the indicated translational constructs. Statistical significance was calculated in relation to non-transgenic controls (values not shown) for each transgenic line. $n > 100$, *$p<0.05$, ***$p<0.001$, ****$p<0.0001$, n.s., not significant (one-way ANOVA followed by Tukey's multiple-comparison test). Three independent lines for each transgene (indicated by #) were analyzed.

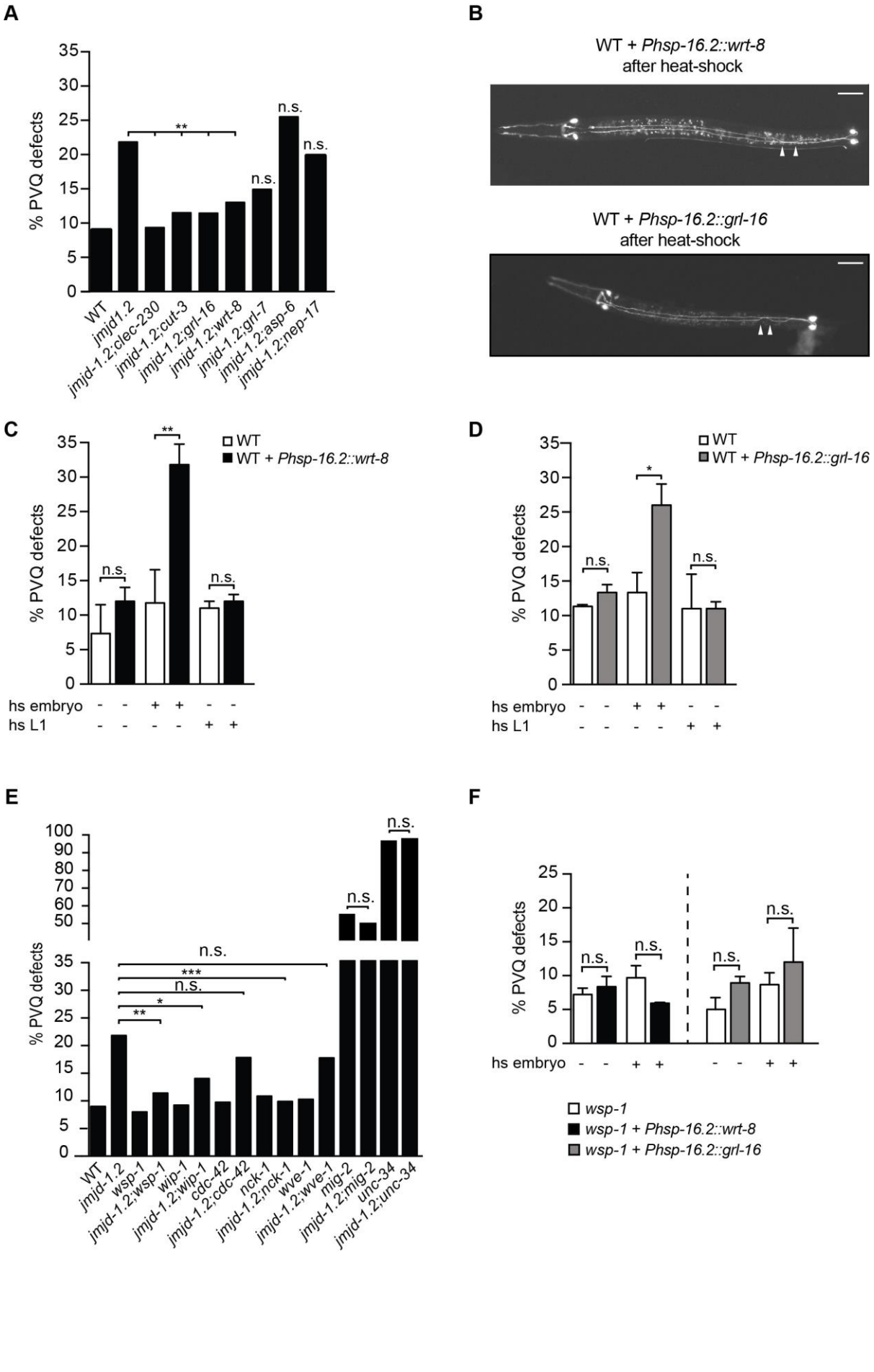

Fig. 4. Axon guidance defects after overexpression of Hedgehog-like proteins are mediated by actin remodeling. A. Quantification of PVQ axonal cross-over defects in the indicated strains. $n > 100$. **B.** Representative images of wild-type young larvae carrying translational constructs for WRT-8 or GRL-16 under the control of a heat-shock (*Phsp-16.2*) promoter, after heat-shock at embryonic stage. PVQ neurons are visualized using the *oyIs14* transgene. Arrowheads indicate the points of axonal cross-over. Ventral view, anterior to the left. Scale bar, 20 μm. **C** and **D.** Quantification of PVQ axonal cross-over defects in wild-type (WT) animals carrying translational constructs for WRT-8 (B) and GRL-16 (C) expressed under the control of a heat-shock (*Phsp-16.2*) promoter, before and after heat-shock at embryonic or L1 larval stages. $n > 100$. **E.** Quantification of PVQ axonal cross-over defects in the indicated strains. $n > 150$. **F.** Quantification of PVQ axonal cross-over defects in *wsp-1(gm324)* mutants carrying translational constructs for WRT-8 or GRL-16 expressed under the control of a heat-shock (*Phsp-16.2*) promoter, before and after heat-shock at embryonic stages. $n > 150$. In all graphs $*p<0.05$, $**p<0.01$, $***p<0.001$, n.s., not significant (one-way ANOVA followed by Tukey's multiple-comparison test). The results in C, D and F are from three independent experiments and error bars represent standard error of proportion.

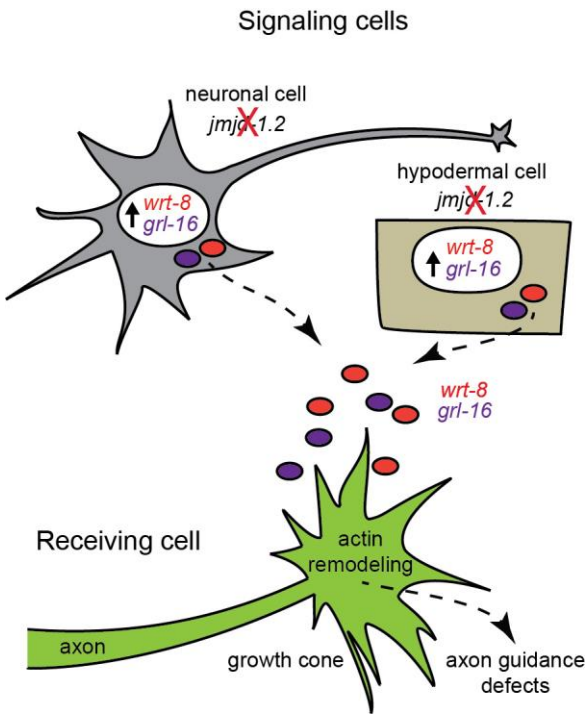

Fig. 5. Proposed model of action of *jmjd-1.2* as a negative transcriptional regulator of Hedgehog-related genes *wrt-8* and *grl-16*. Upon loss of *jmjd-1.2*, unidentified hypodermal cells and neurons (signaling cells) secrete aberrantly high levels of WRT-8 and GRL-16, causing axon guidance defects in receiving cells (e.g. PVQs) by impairing proper actin cytoskeleton remodeling at the growth cone.

SUPPLEMENTARY INFORMATION

SUPPLEMENTARY MATERIALS AND METHODS

Generation of transgenic constructs

To generate *jmjd-1.2_JmjCmut::GFP*, *jmjd-1.2_XLMR::GFP* and *jmjd-1.2_PHDmut::GFP* constructs, the original vector containing *jmjd-1.2::GFP* was mutated using the QuikChange Site-Directed Mutagenesis Kit (Stratagene). Specifically, for *jmjd-1.2 JmjCmut::GFP*, the histidine at position 508 (H508) and the valine at position 509 (V509) were changed to leucine and glutamic acid, respectively, using the primers Fw (GCTGGATCTTATACGGATTTCCTCGAGGACTTTGGTGGTAGTAGC) and Rv (GCTACTACCACCAAAGTCCTCGAGGAAATCCGTATAAGATCCAGC). For *jmjd-1.2_XLMR::GFP*, the phenylalanine at position 507 (F507) was changed to serine using the primers XLMR_Fw (GGATCTTATACGGATTCCCACGTGGAC) and XLMR_Rv (GTCCACGTGGGAATCCGTATAAGATCC). For *jmjd-1.2_PHDmut::GFP*, the glycine at position 254 (G254) was changed to alanine using the primers PHD_G254A_Fw (TTCCAATGGATTGCCTGTGACTCTTGCC) and PHD_G254A_Rv (GGCAAGAGTCACAGGCAATCCATTGGAA).

For overexpression experiments, the heat-shock promoter *hsp-16.2* was PCR-amplified from N2 genomic DNA using the primers Phsp-16.2_GW_fw (GGGGACAACTTTGTATAGAAAAGTTGtttcgaagtttttagatgcact) and Phsp-16.2_GW_rv (GGGGACTGCTTTTTTGTACAAACTTGgattatagtttgaagatttctaatt), and cloned into pDONR P4-P1R vector. The genomic regions of *wrt-8* (2,350 bp, *C29F3.2* in WormBase) and *grl-16* (2,627 bp, *Y65B4BR.6* in WormBase) were PCR-amplified from N2 genomic DNA using the primers wrt-8_fw (ATGAATTATTTATTACTGGTATCTGG) / wrt-8_rv (GTAGGAAATCATTTTCGATGGCA) and grl-16_fw (ATGAGAGTCTTGGTAGCCGTC) / grl-16_rv (ATCCTCCCAGGTAAGCGAGT), respectively. The resulting fragments were inserted into pDONR pCR8 vector and the final plasmids expressing *Phsp-16.2::wrt-8::GFP* and *Phsp-16.2::grl-16::GFP* were constructed using MultiSite Gateway Three-Fragment Vector Construction Kit.

Table S1. Transgenic and non-transgenic siblings analyzed for rescue experiments

Strain	Genotype	Defects observed (%)
ZR111	*jmjd-1.2(tm3713); oyIs14; zrEx26 Ex(Pjmjd-1.2::jmjd-1.2::GFP)*	12
ZR111	*jmjd-1.2(tm3713); oyIs14* (non-transgenic siblings)	21
ZR109	*jmjd-1.2(tm3713); oyIs14; zrEx35 Ex(Prab-3::jmjd-1.2::GFP)*	9
ZR109	*jmjd-1.2(tm3713); oyIs14* (non-transgenic siblings)	23
ZR551	*jmjd-1.2(tm3713); oyIs14; zrEx150 Ex(Pdpy-7::jmjd-1.2::GFP)*	14
ZR551	*jmjd-1.2(tm3713); oyIs14* (non-transgenic siblings)	25
ZR155	*jmjd-1.2(tm3713); oyIs14; zrEx37 Ex(Pmyo-3::jmjd-1.2::GFP)*	19
ZR155	*jmjd-1.2(tm3713); oyIs14* (non-transgenic siblings)	20
ZR550	*jmjd-1.2(tm3713); oyIs14; zrEx149 Ex(Psra-6::jmjd-1.2::GFP)*	19
ZR550	*jmjd-1.2(tm3713); oyIs14* (non-transgenic siblings)	21
ZR984	*jmjd-1.2(tm3713); oyIs14; zrEx359 Ex(Podr-2::jmjd-1.2::GFP)*	23
ZR984	*jmjd-1.2(tm3713); oyIs14* (non-transgenic siblings)	22
ZR148	*jmjd-1.2(tm3713); oyIs14; zrEx33 Ex(Pjmjd-1.2::jmjd-1.2_JmjCmut::GFP)*	26
ZR148	*jmjd-1.2(tm3713); oyIs14* (non-transgenic siblings)	24
ZR894	*jmjd-1.2(tm3713); oyIs14; zrEx317 Ex(Pjmjd-1.2::jmjd-1.2_ XLMR::GFP)*	20
ZR894	*jmjd-1.2(tm3713); oyIs14* (non-transgenic siblings)	22
ZR955	*jmjd-1.2(tm3713); oyIs14; zrEx356 Ex(Pjmjd-1.2::jmjd-1.2_ PHDmut::GFP)*	27
ZR955	*jmjd-1.2(tm3713); oyIs14* (non-transgenic siblings)	20

Quantification of PVQ axonal cross-over defects in the indicated strains. $n > 50$ for each strain.

Table S2. Loss of either *clec-230*, *cut-3*, *grl-16* or *wrt-8* restores correct PVQ guidance in *jmjd-1.2(tm3713)* mutants

Genotype	Defects observed (%)
WT	9 (*n*=267)
jmjd-1.2(tm3713)	22 (*n*=286)
clec-230(ok3131)	12 (*n*=209)
jmjd-1.2(tm3713);clec-230(ok3131)	9 (*n*=187) **
cut-3(ok1819)	13 (*n*=136)
jmjd-1.2(tm3713);cut-3(ok1819)	12 (*n*=158) **
grl-16(ok2959)	16 (*n*=215)
jmjd-1.2(tm3713);grl-16(ok2959)	12 (*n*=217) **
wrt-8(tm1585)	12 (*n*=201)
jmjd-1.2(tm3713);wrt-8(tm1585)	13 (*n*=326) **
grl-7(ok2644)	12 (*n*=129)
jmjd-1.2(tm3713);grl-7(ok2644)	16 (*n*=185) n.s.
asp-6(tm2213)	26 (*n*=215)
jmjd-1.2(tm3713);asp-6(tm2213)	25 (*n*=150) n.s.
nep-17(ok3251)	74 (*n*=184)
jmjd-1.2(tm3713);nep-17(ok3251)	20 (n=120) n.s.

Quantification of PVQ axonal cross-over defects in the indicated strains. *n* = number of analyzed animals. **$p<0.01$, n.s., not significant (one-way ANOVA followed by Tukey's multiple-comparison test).

Table S3. Mammalian components of the Hedgehog pathway and their *C. elegans* homologs

Mammalian gene	*C. elegans* homolog	Description
Shh, Ihh, Dhh	*wrt, grl, grd, qua-1, hog-1*	Ligands
Skn/HHAT	*hhat-1, hhat-2*	Ligand modulator (palmitoylation)
DISP	*che-14, ptd-2*	Secretion of ligands (12-Pass TM)
EXT1	*rib-1*	Trafficking/diffusion of ligands
EXTL3	*rib-2*	Trafficking/diffusion of ligands
Glypican-6	*gpn-1*	Trafficking/diffusion of ligands
PTCH1, PTCH2	*ptc-1, ptc-3*	Ligand receptors
GAS1	*phg-1*	Co-receptor
LRP2	*lrp-1*	Co-receptor
HHIP	-	Hedgehog interacting protein
SMO	-	GPC receptor
FU	-	Serine/threonine kinase
SUFU	-	Sufu domain
KIF27, KIF7	-	Kinesin-like
Gli1, Gli2, Gli3	*tra-1*	Zinc finger transcription factors

List of genes encoding components of the Hedgehog pathway in mammals, homologs in *C. elegans* and brief description of their functions.

Table S4. Transgenic strains

Strain	Genotype
ZR111	*jmjd-1.2(tm3713); oyIs14; zrEx26 Ex(Pjmjd-1.2::jmjd-1.2::GFP)*
ZR526	*jmjd-1.2(tm3713); oyIs14; zrEx137 Ex(Pjmjd-1.2::jmjd-1.2::GFP)*
ZR527	*jmjd-1.2(tm3713); oyIs14; zrEx138 Ex(Pjmjd-1.2::jmjd-1.2::GFP)*
ZR109	*jmjd-1.2(tm3713); oyIs14; zrEx12 Ex(Prab-3::jmjd-1.2::GFP)*
ZR153	*jmjd-1.2(tm3713); oyIs14; zrEx35 Ex(Prab-3::jmjd-1.2::GFP)*
ZR259	*jmjd-1.2(tm3713); oyIs14; zrEx53 Ex(Prab-3::jmjd-1.2::GFP)*
ZR551	*jmjd-1.2(tm3713); oyIs14; zrEx150 Ex(Pdpy-7::jmjd-1.2::GFP)*
ZR552	*jmjd-1.2(tm3713); oyIs14; zrEx151 Ex(Pdpy-7::jmjd-1.2::GFP)*
ZR553	*jmjd-1.2(tm3713); oyIs14; zrEx152 Ex(Pdpy-7::jmjd-1.2::GFP)*
ZR718	*jmjd-1.2(tm3713); oyIs14; zrEx251 Ex(Prab-3::jmjd-1.2::GFP); Ex(Pdpy-7::jmjd-1.2::GFP)*
ZR719	*jmjd-1.2(tm3713); oyIs14; zrEx252 Ex(Prab-3::jmjd-1.2::GFP); Ex(Pdpy-7::jmjd-1.2::GFP)*
ZR720	*jmjd-1.2(tm3713); oyIs14; zrEx253 Ex(Prab-3::jmjd-1.2::GFP); Ex(Pdpy-7::jmjd-1.2::GFP)*
ZR155	*jmjd-1.2(tm3713); oyIs14; zrEx37 Ex(Pmyo-3::jmjd-1.2::GFP)*
ZR183	*jmjd-1.2(tm3713); oyIs14; zrEx40 Ex(Pmyo-3::jmjd-1.2::GFP)*
ZR184	*jmjd-1.2(tm3713); oyIs14; zrEx41 Ex(Pmyo-3::jmjd-1.2::GFP)*
ZR550	*jmjd-1.2(tm3713); oyIs14; zrEx149 Ex(Psra-6::jmjd-1.2::GFP)*
ZR712	*jmjd-1.2(tm3713); oyIs14; zrEx249 Ex(Psra-6::jmjd-1.2::GFP)*
ZR713	*jmjd-1.2(tm3713); oyIs14; zrEx250 Ex(Psra-6::jmjd-1.2::GFP)*
ZR984	*jmjd-1.2(tm3713); oyIs14; zrEx359 Ex(Podr-2::jmjd-1.2::GFP)*
ZR985	*jmjd-1.2(tm3713); oyIs14; zrEx360 Ex(Podr-2::jmjd-1.2::GFP)*
ZR986	*jmjd-1.2(tm3713); oyIs14; zrEx361 Ex(Podr-2::jmjd-1.2::GFP)*

Strain	Genotype
ZR148	*jmjd-1.2(tm3713); oyIs14; zrEx33 Ex(Pjmjd-1.2::jmjd-1.2_ JmjCmut::GFP)*
ZR952	*jmjd-1.2(tm3713); oyIs14; zrEx353 Ex(Pjmjd-1.2::jmjd-1.2_ JmjCmut::GFP)*
ZR953	*jmjd-1.2(tm3713); oyIs14; zrEx354 Ex(Pjmjd-1.2::jmjd-1.2_ JmjCmut::GFP)*
ZR894	*jmjd-1.2(tm3713); oyIs14; zrEx317 Ex(Pjmjd-1.2::jmjd-1.2_ XLMR::GFP)*
ZR895	*jmjd-1.2(tm3713); oyIs14; zrEx318 Ex(Pjmjd-1.2::jmjd-1.2_ XLMR::GFP)*
ZR896	*jmjd-1.2(tm3713); oyIs14; zrEx319 Ex(Pjmjd-1.2::jmjd-1.2_ XLMR::GFP)*
ZR954	*jmjd-1.2(tm3713); oyIs14; zrEx355 Ex(Pjmjd-1.2::jmjd-1.2_ PHDmut::GFP)*
ZR955	*jmjd-1.2(tm3713); oyIs14; zrEx356 Ex(Pjmjd-1.2::jmjd-1.2_ PHDmut::GFP)*
ZR956	*jmjd-1.2(tm3713); oyIs14; zrEx357 Ex(Pjmjd-1.2::jmjd-1.2_ PHDmut::GFP)*
ZR942	*oyIs14; zrEx349 Ex(Phsp-16.2::wrt-8::GFP)*
ZR943	*oyIs14; zrEx350 Ex(Phsp-16.2::wrt-8::GFP)*
ZR944	*oyIs14; zrEx351 Ex(Phsp-16.2::wrt-8::GFP)*
ZR945	*oyIs14; zrEx352 Ex(Phsp-16.2::grl-16::GFP)*
ZR1014	*wsp-1(gm324); oyIs14; zrEx351 Ex(Phsp-16.2::wrt-8::GFP)*
ZR1015	*wsp-1(gm324); oyIs14; zrEx352 Ex(Phsp-16.2::grl-16::GFP)*

List of transgenic strains used in this study: names and genotypes are indicated.

SUPPLEMENTARY FIGURES

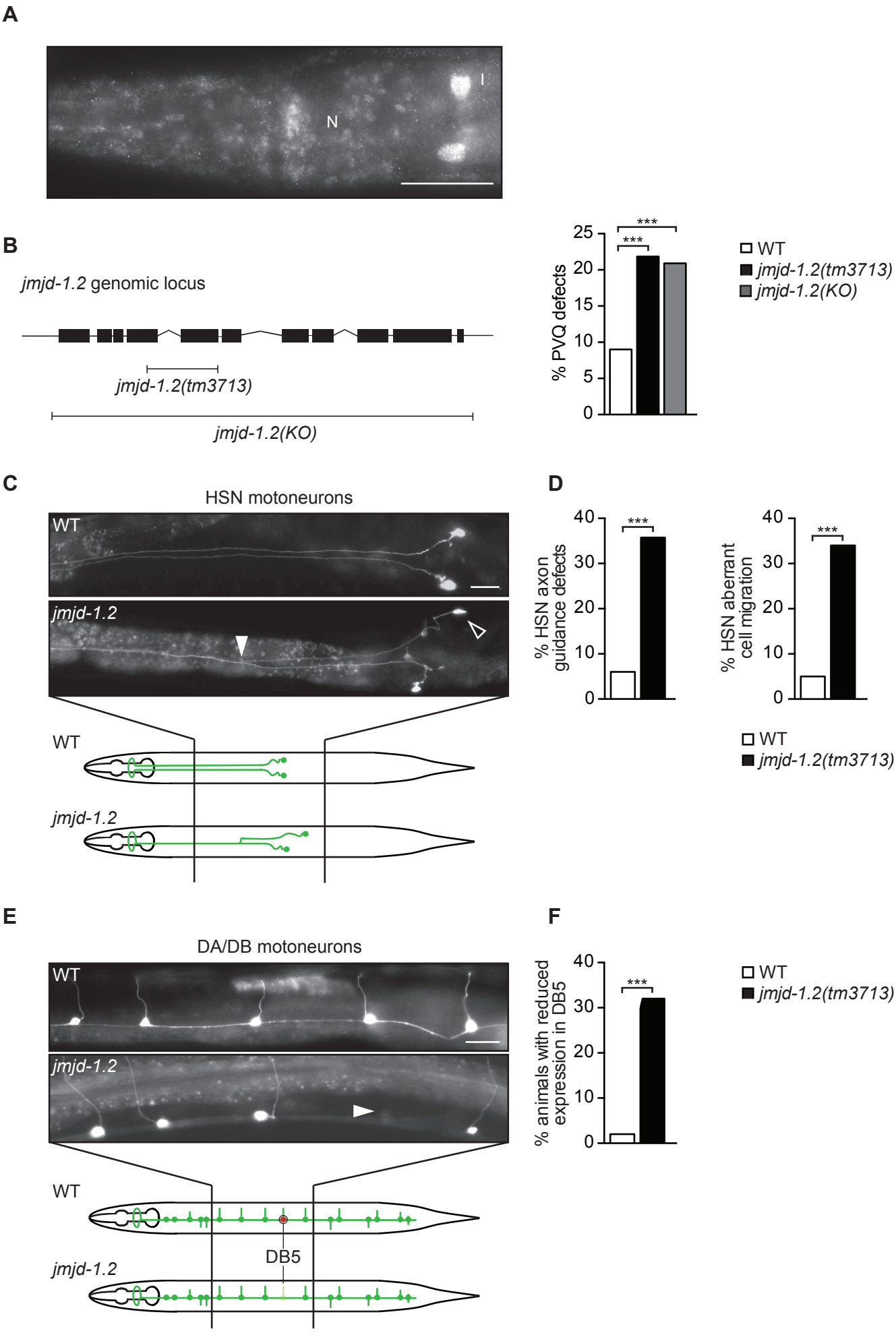

Fig. S1. *jmjd-1.2(tm3713)* animals display distinct neuronal defects. **A.** Large-sized image of a wild-type animal fixed and stained with JMJD-1.2 antibody. N, neurons; I, intestinal cells. Ventral view, anterior to the left. Scale bar, 20 µm. **B.** Left: Genomic organization of *jmjd-1.2*. Black H-shaped lines indicate the position of the *tm3713* and the *(KO)* deletion. Right: Quantification of PVQ axonal cross-over defects in *jmjd-1.2(tm3713)* and *jmjd-1.2(KO)* animals, expressed as percentages of defects. $n > 200$, ***$p<0.001$ (Fisher's exact test). **C.** Top: Representative images of HSN motoneurons in wild-type (WT) and *jmjd-1.2(tm3713)* adult animals. The white arrowhead indicates the point of axonal cross-over and the empty arrowhead indicates aberrant position of the cell body. Ventral view, anterior to the left. Scale bar, 20 µm. Bottom: Schematic diagrams of HSN motoneurons in wild-type and *jmjd-1.2(tm3713)* animals. **D.** Left: Quantification of HSN axonal cross-over defects in *jmjd-1.2(tm3713)* animals. Right: Quantification of HSN aberrant cell migration in *jmjd-1.2(tm3713)* adult animals. $n > 100$, ***$p<0.001$ (Fisher's exact test). **E.** Top: Representative images of DA/DB motoneurons in wild-type and *jmjd-1.2(tm3713)* adult animals. The white arrowhead indicates reduced expression of the transgene in DB5 cell body. Ventral view, anterior to the left. Scale bar, 20 µm. Bottom: Schematic diagrams of DA/DB motoneurons in wild-type and *jmjd-1.2(tm3713)* animals. **F.** Quantification of animals with reduced expression of *evIs82b* in DB5 in wild-type and *jmjd-1.2(tm3713)* strains. $n > 100$, ***$p<0.001$ (Fisher's exact test).

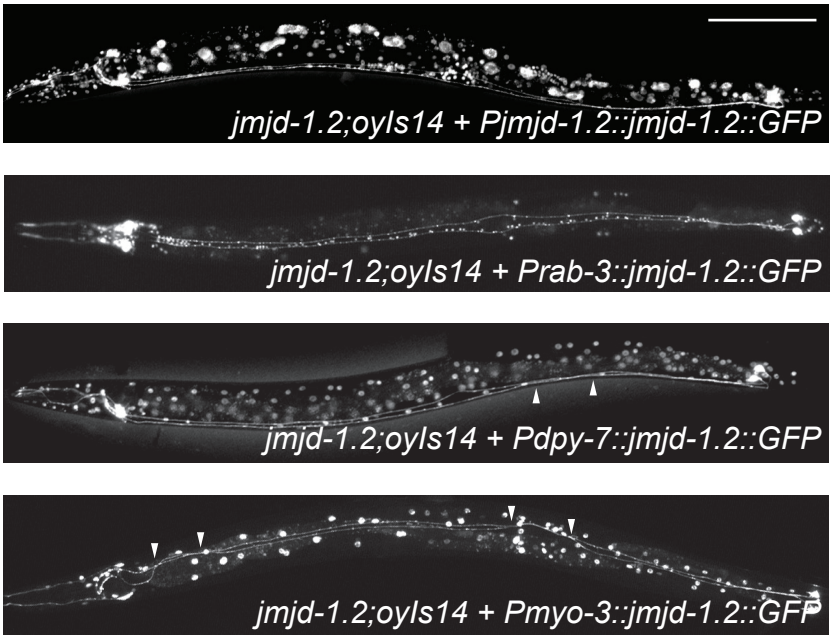

Fig. S2. Expression patterns of animals analyzed for rescue experiments. Representative images of *jmjd-1.2(tm3713);oyIs14* adult animals expressing the construct *jmjd-1.2::GFP* under the control of *jmjd-1.2* promoter (*Pjmjd-1.2*) or different tissue-specific promoters: *Prab-3*, nervous system; *Pdpy*-7, hypodermis; *Pmyo-3*, body wall muscles. In all images, anterior is to the left. Animals expressing *Pjmjd-1.2::jmjd-1.2* and *Pdpy-7::jmjd-1.2* are in lateral position, the others in ventral position. Scale bar, 100 µm.

A

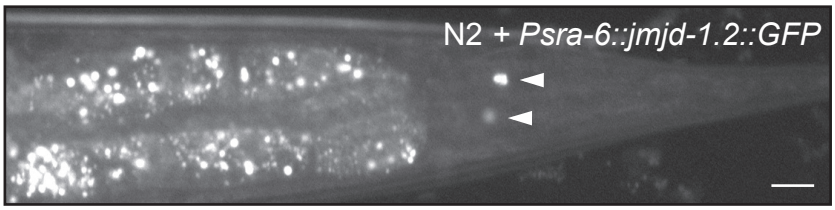

B

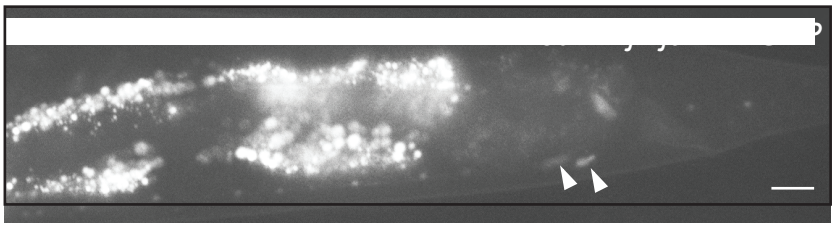

C

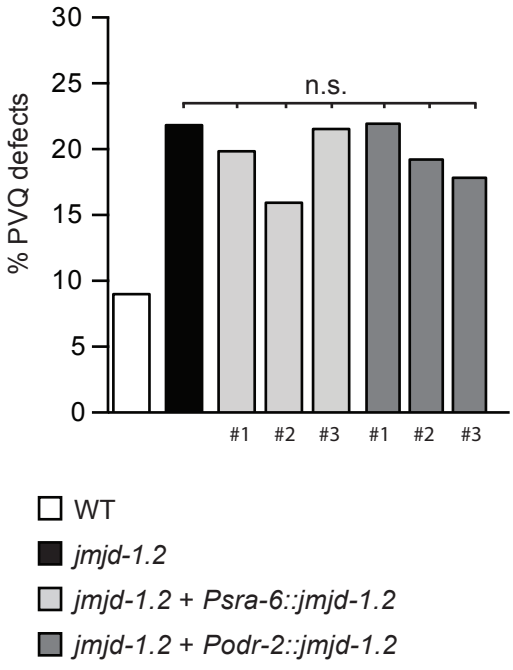

Fig. S3. The activity of *jmjd-1.2* is not cell-autonomous. **A.** Representative image of a wild-type adult animal expressing the construct *jmjd-1.2::GFP* under the control of the *sra-6* promoter (*Psra-6*), expressed in PVQs. Ventral view, anterior to the left. Arrowheads indicate the PVQ cellular bodies. Scale bar, 10 µm. **B.** Representative image of a wild-type adult animal expressing the construct *jmjd-1.2::GFP* under the control of the *odr-2* promoter (*Podr-2*), expressed in PVPs. Ventral view, anterior to the left. Arrowheads indicate the PVP cellular bodies. Scale bar, 10 µm. **C.** Quantification of PVQ axonal cross-over defects in *jmjd-1.2(tm3713)* mutants expressing transgenic JMJD-1.2 specifically in PVQs or in PVPs. $n > 100$, n.s., not significant (one-way ANOVA followed by Tukey's multiple-comparison test). Three independent lines for each transgene (indicated by #) were analyzed.

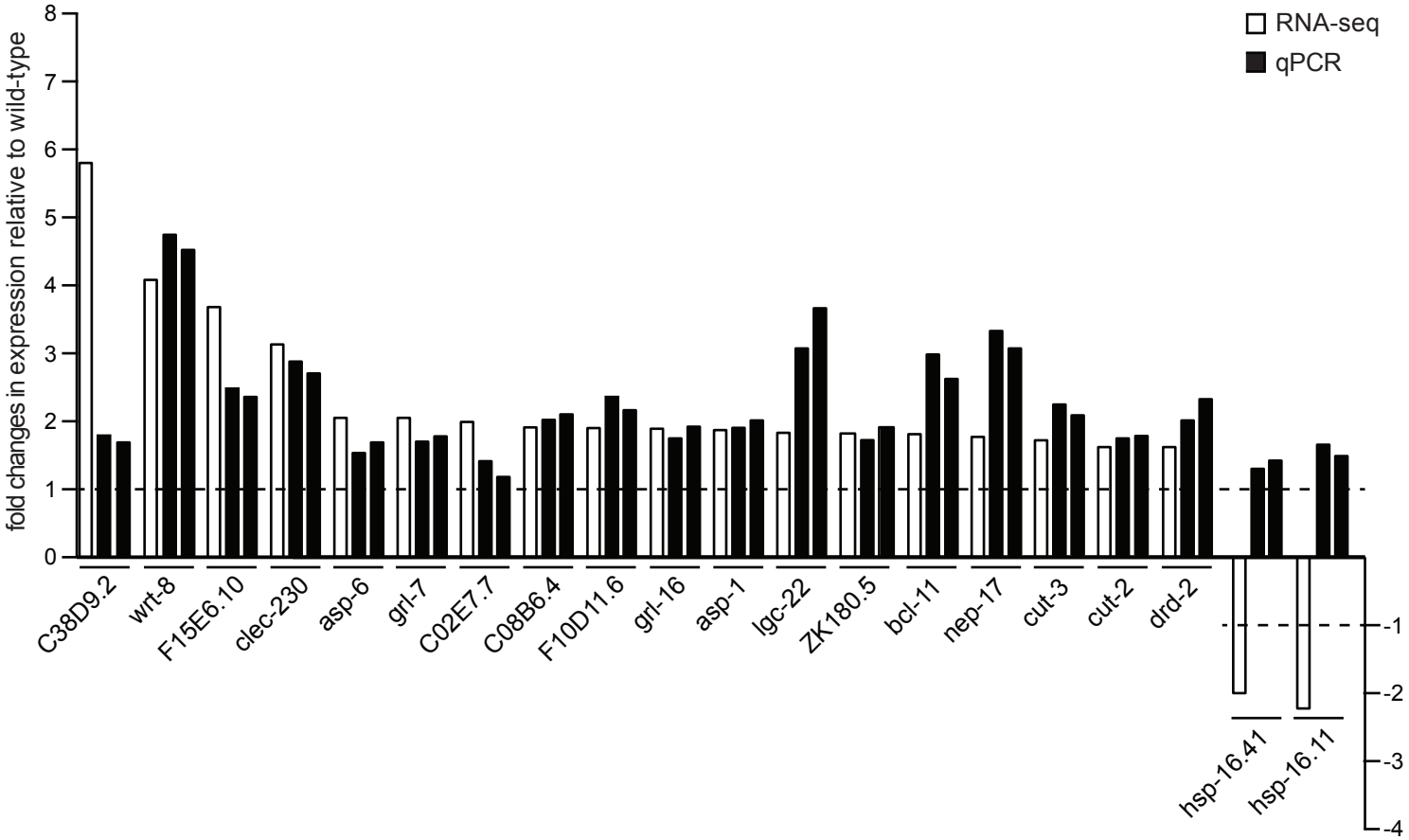

Fig. S4. qPCR validation of genes found deregulated in *jmjd-1.2(tm3713)* embryos by RNA-sequencing. Expression of indicated genes in *jmjd-1.2(tm3713)* embryos is reported as fold change relative to wild-type. Dashed bars are set to ±1. Deregulation of *C38D9.2*, *C02E7.7*, *hsp-16.41* and *hsp-16.11* was not confirmed by qPCR.

SUPPLEMENTARY INFORMATION

SUPPLEMENTARY MATERIALS AND METHODS

Generation of transgenic constructs

To generate *jmjd-1.2_JmjCmut::GFP*, *jmjd-1.2_XLMR::GFP* and *jmjd-1.2_PHDmut::GFP* constructs, the original vector containing *jmjd-1.2::GFP* was mutated using the QuikChange Site-Directed Mutagenesis Kit (Stratagene). Specifically, for *jmjd-1.2 JmjCmut::GFP*, the histidine at position 508 (H508) and the valine at position 509 (V509) were changed to leucine and glutamic acid, respectively, using the primers Fw (GCTGGATCTTATACGGATTTCCTCGAGGACTTTGGTGGTAGTAGC) and Rv (GCTACTACCACCAAAGTCCTCGAGGAAATCCGTATAAGATCCAGC). For *jmjd-1.2_XLMR::GFP*, the phenylalanine at position 507 (F507) was changed to serine using the primers XLMR_Fw (GGATCTTATACGGATTCCCACGTGGAC) and XLMR_Rv (GTCCACGTGGGAATCCGTATAAGATCC). For *jmjd-1.2_PHDmut::GFP*, the glycine at position 254 (G254) was changed to alanine using the primers PHD_G254A_Fw (TTCCAATGGATTGCCTGTGACTCTTGCC) and PHD_G254A_Rv (GGCAAGAGTCACAGGCAATCCATTGGAA).

For overexpression experiments, the heat-shock promoter *hsp-16.2* was PCR-amplified from N2 genomic DNA using the primers Phsp-16.2_GW_fw (GGGGACAACTTTGTATAGAAAAGTTGtttcgaagtttttagatgcact) and Phsp-16.2_GW_rv (GGGGACTGCTTTTTTGTACAAACTTGgattatagtttgaagatttctaatt), and cloned into pDONR P4-P1R vector. The genomic regions of *wrt-8* (2,350 bp, *C29F3.2* in WormBase) and *grl-16* (2,627 bp, *Y65B4BR.6* in WormBase) were PCR-amplified from N2 genomic DNA using the primers wrt-8_fw (ATGAATTATTTATTACTGGTATCTGG) / wrt-8_rv (GTAGGAAATCATTTTCGATGGCA) and grl-16_fw (ATGAGAGTCTTGGTAGCCGTC) / grl-16_rv (ATCCTCCCAGGTAAGCGAGT), respectively. The resulting fragments were inserted into pDONR pCR8 vector and the final plasmids expressing *Phsp-16.2::wrt-8::GFP* and *Phsp-16.2::grl-16::GFP* were constructed using MultiSite Gateway Three-Fragment Vector Construction Kit.

Table S1. Transgenic and non-transgenic siblings analyzed for rescue experiments

Strain	Genotype	Defects observed (%)
ZR111	*jmjd-1.2(tm3713); oyIs14; zrEx26 Ex(Pjmjd-1.2::jmjd-1.2::GFP)*	12
ZR111	*jmjd-1.2(tm3713); oyIs14* (non-transgenic siblings)	21
ZR109	*jmjd-1.2(tm3713); oyIs14; zrEx35 Ex(Prab-3::jmjd-1.2::GFP)*	9
ZR109	*jmjd-1.2(tm3713); oyIs14* (non-transgenic siblings)	23
ZR551	*jmjd-1.2(tm3713); oyIs14; zrEx150 Ex(Pdpy-7::jmjd-1.2::GFP)*	14
ZR551	*jmjd-1.2(tm3713); oyIs14* (non-transgenic siblings)	25
ZR155	*jmjd-1.2(tm3713); oyIs14; zrEx37 Ex(Pmyo-3::jmjd-1.2::GFP)*	19
ZR155	*jmjd-1.2(tm3713); oyIs14* (non-transgenic siblings)	20
ZR550	*jmjd-1.2(tm3713); oyIs14; zrEx149 Ex(Psra-6::jmjd-1.2::GFP)*	19
ZR550	*jmjd-1.2(tm3713); oyIs14* (non-transgenic siblings)	21
ZR984	*jmjd-1.2(tm3713); oyIs14; zrEx359 Ex(Podr-2::jmjd-1.2::GFP)*	23
ZR984	*jmjd-1.2(tm3713); oyIs14* (non-transgenic siblings)	22
ZR148	*jmjd-1.2(tm3713); oyIs14; zrEx33 Ex(Pjmjd-1.2::jmjd-1.2_JmjCmut::GFP)*	26
ZR148	*jmjd-1.2(tm3713); oyIs14* (non-transgenic siblings)	24
ZR894	*jmjd-1.2(tm3713); oyIs14; zrEx317 Ex(Pjmjd-1.2::jmjd-1.2_ XLMR::GFP)*	20
ZR894	*jmjd-1.2(tm3713); oyIs14* (non-transgenic siblings)	22
ZR955	*jmjd-1.2(tm3713); oyIs14; zrEx356 Ex(Pjmjd-1.2::jmjd-1.2_ PHDmut::GFP)*	27
ZR955	*jmjd-1.2(tm3713); oyIs14* (non-transgenic siblings)	20

Quantification of PVQ axonal cross-over defects in the indicated strains. $n > 50$ for each strain.

Table S2. Loss of either *clec-230*, *cut-3*, *grl-16* or *wrt-8* restores correct PVQ guidance in *jmjd-1.2(tm3713)* mutants

Genotype	Defects observed (%)
WT	9 (*n*=267)
jmjd-1.2(tm3713)	22 (*n*=286)
clec-230(ok3131)	12 (*n*=209)
jmjd-1.2(tm3713);clec-230(ok3131)	9 (*n*=187) **
cut-3(ok1819)	13 (*n*=136)
jmjd-1.2(tm3713);cut-3(ok1819)	12 (*n*=158) **
grl-16(ok2959)	16 (*n*=215)
jmjd-1.2(tm3713);grl-16(ok2959)	12 (*n*=217) **
wrt-8(tm1585)	12 (*n*=201)
jmjd-1.2(tm3713);wrt-8(tm1585)	13 (*n*=326) **
grl-7(ok2644)	12 (*n*=129)
jmjd-1.2(tm3713);grl-7(ok2644)	16 (*n*=185) n.s.
asp-6(tm2213)	26 (*n*=215)
jmjd-1.2(tm3713);asp-6(tm2213)	25 (*n*=150) n.s.
nep-17(ok3251)	74 (*n*=184)
jmjd-1.2(tm3713);nep-17(ok3251)	20 (n=120) n.s.

Quantification of PVQ axonal cross-over defects in the indicated strains. *n* = number of analyzed animals. **$p<0.01$, n.s., not significant (one-way ANOVA followed by Tukey's multiple-comparison test).

Table S3. Mammalian components of the Hedgehog pathway and their *C. elegans* homologs

Mammalian gene	*C. elegans* homolog	Description
Shh, Ihh, Dhh	*wrt, grl, grd, qua-1, hog-1*	Ligands
Skn/HHAT	*hhat-1, hhat-2*	Ligand modulator (palmitoylation)
DISP	*che-14, ptd-2*	Secretion of ligands (12-Pass TM)
EXT1	*rib-1*	Trafficking/diffusion of ligands
EXTL3	*rib-2*	Trafficking/diffusion of ligands
Glypican-6	*gpn-1*	Trafficking/diffusion of ligands
PTCH1, PTCH2	*ptc-1, ptc-3*	Ligand receptors
GAS1	*phg-1*	Co-receptor
LRP2	*lrp-1*	Co-receptor
HHIP	-	Hedgehog interacting protein
SMO	-	GPC receptor
FU	-	Serine/threonine kinase
SUFU	-	Sufu domain
KIF27, KIF7	-	Kinesin-like
Gli1, Gli2, Gli3	*tra-1*	Zinc finger transcription factors

List of genes encoding components of the Hedgehog pathway in mammals, homologs in *C. elegans* and brief description of their functions.

Table S4. Transgenic strains

Strain	Genotype
ZR111	*jmjd-1.2(tm3713); oyIs14; zrEx26 Ex(Pjmjd-1.2::jmjd-1.2::GFP)*
ZR526	*jmjd-1.2(tm3713); oyIs14; zrEx137 Ex(Pjmjd-1.2::jmjd-1.2::GFP)*
ZR527	*jmjd-1.2(tm3713); oyIs14; zrEx138 Ex(Pjmjd-1.2::jmjd-1.2::GFP)*
ZR109	*jmjd-1.2(tm3713); oyIs14; zrEx12 Ex(Prab-3::jmjd-1.2::GFP)*
ZR153	*jmjd-1.2(tm3713); oyIs14; zrEx35 Ex(Prab-3::jmjd-1.2::GFP)*
ZR259	*jmjd-1.2(tm3713); oyIs14; zrEx53 Ex(Prab-3::jmjd-1.2::GFP)*
ZR551	*jmjd-1.2(tm3713); oyIs14; zrEx150 Ex(Pdpy-7::jmjd-1.2::GFP)*
ZR552	*jmjd-1.2(tm3713); oyIs14; zrEx151 Ex(Pdpy-7::jmjd-1.2::GFP)*
ZR553	*jmjd-1.2(tm3713); oyIs14; zrEx152 Ex(Pdpy-7::jmjd-1.2::GFP)*
ZR718	*jmjd-1.2(tm3713); oyIs14; zrEx251 Ex(Prab-3::jmjd-1.2::GFP); Ex(Pdpy-7::jmjd-1.2::GFP)*
ZR719	*jmjd-1.2(tm3713); oyIs14; zrEx252 Ex(Prab-3::jmjd-1.2::GFP); Ex(Pdpy-7::jmjd-1.2::GFP)*
ZR720	*jmjd-1.2(tm3713); oyIs14; zrEx253 Ex(Prab-3::jmjd-1.2::GFP); Ex(Pdpy-7::jmjd-1.2::GFP)*
ZR155	*jmjd-1.2(tm3713); oyIs14; zrEx37 Ex(Pmyo-3::jmjd-1.2::GFP)*
ZR183	*jmjd-1.2(tm3713); oyIs14; zrEx40 Ex(Pmyo-3::jmjd-1.2::GFP)*
ZR184	*jmjd-1.2(tm3713); oyIs14; zrEx41 Ex(Pmyo-3::jmjd-1.2::GFP)*
ZR550	*jmjd-1.2(tm3713); oyIs14; zrEx149 Ex(Psra-6::jmjd-1.2::GFP)*
ZR712	*jmjd-1.2(tm3713); oyIs14; zrEx249 Ex(Psra-6::jmjd-1.2::GFP)*
ZR713	*jmjd-1.2(tm3713); oyIs14; zrEx250 Ex(Psra-6::jmjd-1.2::GFP)*
ZR984	*jmjd-1.2(tm3713); oyIs14; zrEx359 Ex(Podr-2::jmjd-1.2::GFP)*
ZR985	*jmjd-1.2(tm3713); oyIs14; zrEx360 Ex(Podr-2::jmjd-1.2::GFP)*
ZR986	*jmjd-1.2(tm3713); oyIs14; zrEx361 Ex(Podr-2::jmjd-1.2::GFP)*

Strain	Genotype
ZR148	*jmjd-1.2(tm3713); oyIs14; zrEx33 Ex(Pjmjd-1.2::jmjd-1.2_ JmjCmut::GFP)*
ZR952	*jmjd-1.2(tm3713); oyIs14; zrEx353 Ex(Pjmjd-1.2::jmjd-1.2_ JmjCmut::GFP)*
ZR953	*jmjd-1.2(tm3713); oyIs14; zrEx354 Ex(Pjmjd-1.2::jmjd-1.2_ JmjCmut::GFP)*
ZR894	*jmjd-1.2(tm3713); oyIs14; zrEx317 Ex(Pjmjd-1.2::jmjd-1.2_ XLMR::GFP)*
ZR895	*jmjd-1.2(tm3713); oyIs14; zrEx318 Ex(Pjmjd-1.2::jmjd-1.2_ XLMR::GFP)*
ZR896	*jmjd-1.2(tm3713); oyIs14; zrEx319 Ex(Pjmjd-1.2::jmjd-1.2_ XLMR::GFP)*
ZR954	*jmjd-1.2(tm3713); oyIs14; zrEx355 Ex(Pjmjd-1.2::jmjd-1.2_ PHDmut::GFP)*
ZR955	*jmjd-1.2(tm3713); oyIs14; zrEx356 Ex(Pjmjd-1.2::jmjd-1.2_ PHDmut::GFP)*
ZR956	*jmjd-1.2(tm3713); oyIs14; zrEx357 Ex(Pjmjd-1.2::jmjd-1.2_ PHDmut::GFP)*
ZR942	*oyIs14; zrEx349 Ex(Phsp-16.2::wrt-8::GFP)*
ZR943	*oyIs14; zrEx350 Ex(Phsp-16.2::wrt-8::GFP)*
ZR944	*oyIs14; zrEx351 Ex(Phsp-16.2::wrt-8::GFP)*
ZR945	*oyIs14; zrEx352 Ex(Phsp-16.2::grl-16::GFP)*
ZR1014	*wsp-1(gm324); oyIs14; zrEx351 Ex(Phsp-16.2::wrt-8::GFP)*
ZR1015	*wsp-1(gm324); oyIs14; zrEx352 Ex(Phsp-16.2::grl-16::GFP)*

List of transgenic strains used in this study: names and genotypes are indicated.

SUPPLEMENTARY FIGURES

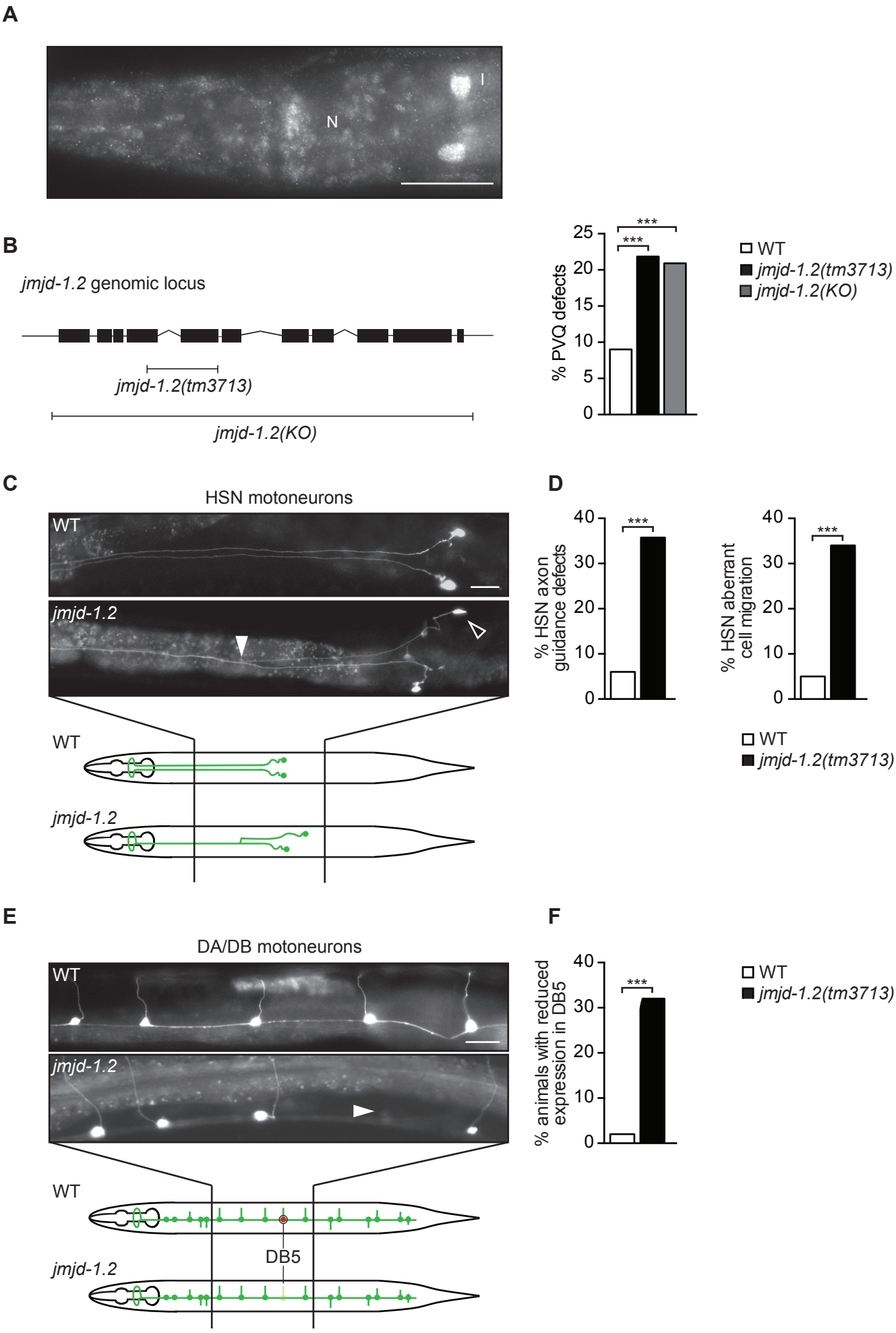

Fig. S1. *jmjd-1.2(tm3713)* animals display distinct neuronal defects. **A.** Large-sized image of a wild-type animal fixed and stained with JMJD-1.2 antibody. N, neurons; I, intestinal cells. Ventral view, anterior to the left. Scale bar, 20 µm. **B.** Left: Genomic organization of *jmjd-1.2*. Black H-shaped lines indicate the position of the *tm3713* and the *(KO)* deletion. Right: Quantification of PVQ axonal cross-over defects in *jmjd-1.2(tm3713)* and *jmjd-1.2(KO)* animals, expressed as percentages of defects. $n > 200$, ***$p<0.001$ (Fisher's exact test). **C.** Top: Representative images of HSN motoneurons in wild-type (WT) and *jmjd-1.2(tm3713)* adult animals. The white arrowhead indicates the point of axonal cross-over and the empty arrowhead indicates aberrant position of the cell body. Ventral view, anterior to the left. Scale bar, 20 µm. Bottom: Schematic diagrams of HSN motoneurons in wild-type and *jmjd-1.2(tm3713)* animals. **D.** Left: Quantification of HSN axonal cross-over defects in *jmjd-1.2(tm3713)* animals. Right: Quantification of HSN aberrant cell migration in *jmjd-1.2(tm3713)* adult animals. $n > 100$, ***$p<0.001$ (Fisher's exact test). **E.** Top: Representative images of DA/DB motoneurons in wild-type and *jmjd-1.2(tm3713)* adult animals. The white arrowhead indicates reduced expression of the transgene in DB5 cell body. Ventral view, anterior to the left. Scale bar, 20 µm. Bottom: Schematic diagrams of DA/DB motoneurons in wild-type and *jmjd-1.2(tm3713)* animals. **F.** Quantification of animals with reduced expression of *evIs82b* in DB5 in wild-type and *jmjd-1.2(tm3713)* strains. $n > 100$, ***$p<0.001$ (Fisher's exact test).

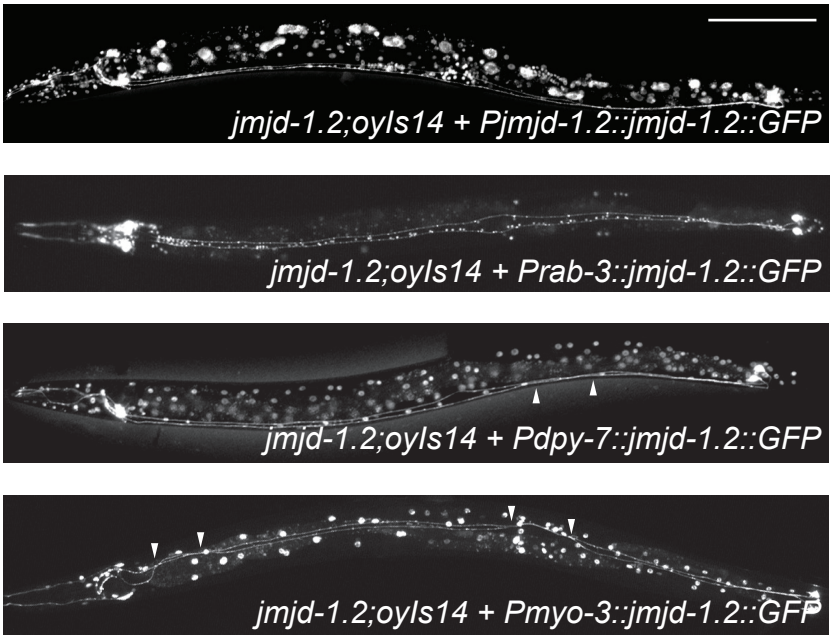

Fig. S2. Expression patterns of animals analyzed for rescue experiments. Representative images of *jmjd-1.2(tm3713);oyIs14* adult animals expressing the construct *jmjd-1.2::GFP* under the control of *jmjd-1.2* promoter (*Pjmjd-1.2*) or different tissue-specific promoters: *Prab-3*, nervous system; *Pdpy*-7, hypodermis; *Pmyo-3*, body wall muscles. In all images, anterior is to the left. Animals expressing *Pjmjd-1.2::jmjd-1.2* and *Pdpy-7::jmjd-1.2* are in lateral position, the others in ventral position. Scale bar, 100 µm.

A

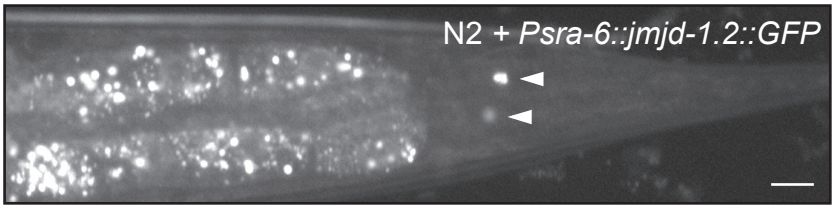

B

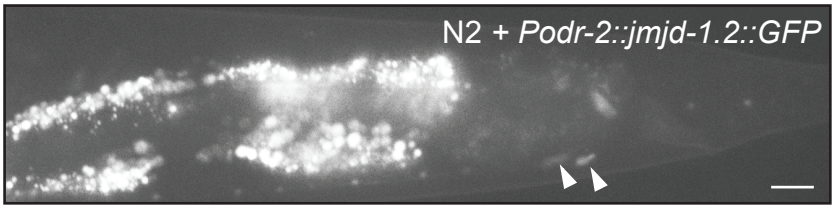

C

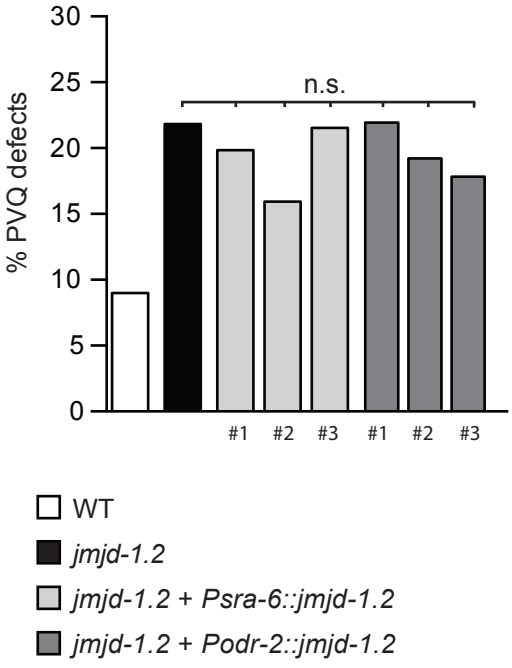

Fig. S3. The activity of *jmjd-1.2* is not cell-autonomous. **A.** Representative image of a wild-type adult animal expressing the construct *jmjd-1.2::GFP* under the control of the *sra-6* promoter (*Psra-6*), expressed in PVQs. Ventral view, anterior to the left. Arrowheads indicate the PVQ cellular bodies. Scale bar, 10 µm. **B.** Representative image of a wild-type adult animal expressing the construct *jmjd-1.2::GFP* under the control of the *odr-2* promoter (*Podr-2*), expressed in PVPs. Ventral view, anterior to the left. Arrowheads indicate the PVP cellular bodies. Scale bar, 10 µm. **C.** Quantification of PVQ axonal cross-over defects in *jmjd-1.2(tm3713)* mutants expressing transgenic JMJD-1.2 specifically in PVQs or in PVPs. $n > 100$, n.s., not significant (one-way ANOVA followed by Tukey's multiple-comparison test). Three independent lines for each transgene (indicated by #) were analyzed.

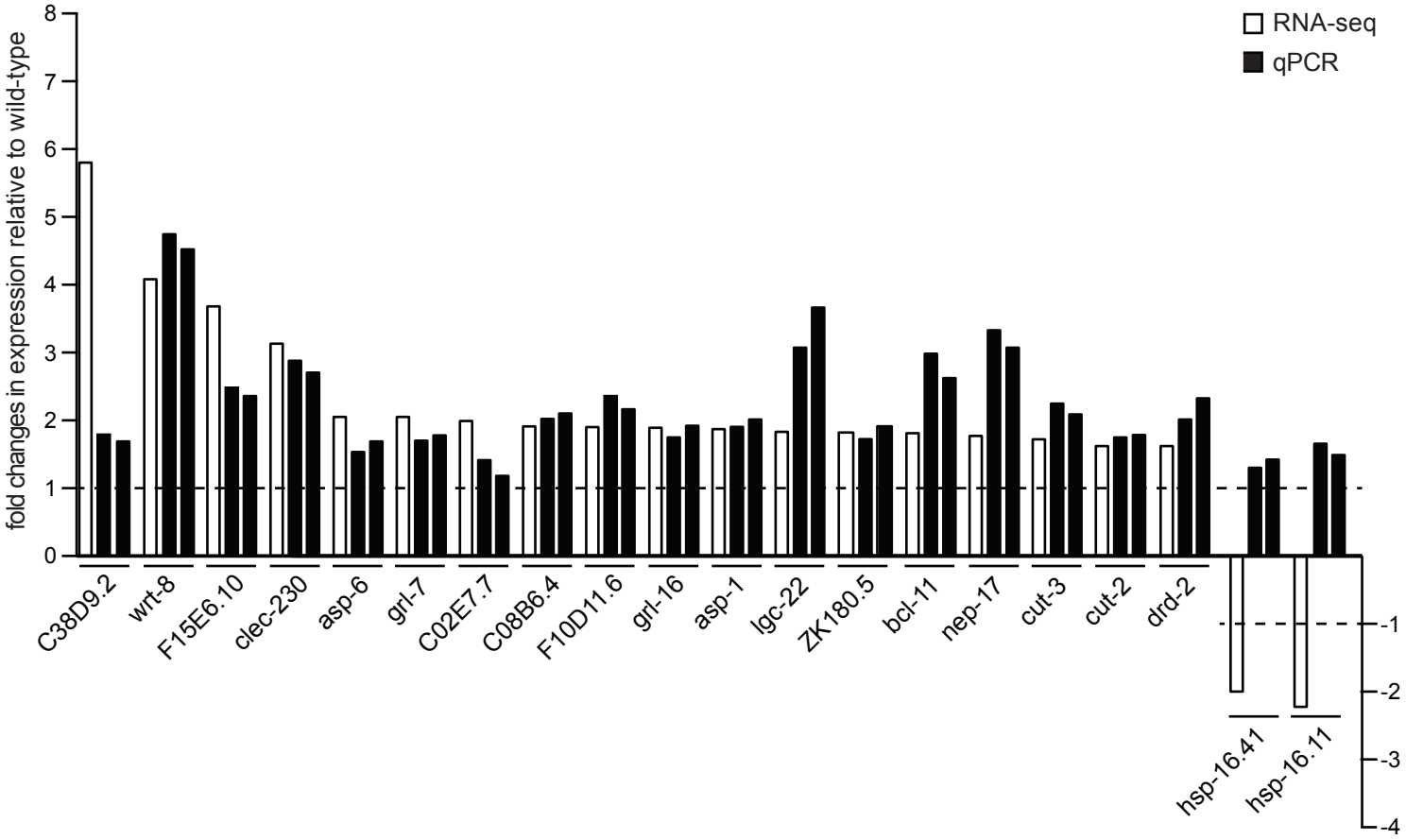

Fig. S4. qPCR validation of genes found deregulated in *jmjd-1.2(tm3713)* embryos by RNA-sequencing. Expression of indicated genes in *jmjd-1.2(tm3713)* embryos is reported as fold change relative to wild-type. Dashed bars are set to ±1. Deregulation of *C38D9.2*, *C02E7.7*, *hsp-16.41* and *hsp-16.11* was not confirmed by qPCR.